Journal Pre-proof

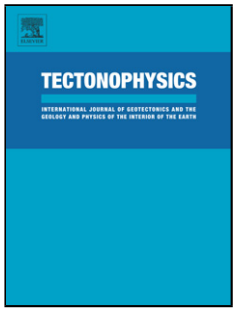

Transient tectonic regimes imposed by megathrust earthquakes and the growth of NW-trending volcanic systems in the Southern Andes

Matteo Lupi, Daniele Trippanera, Diego Gonzalez, Sebastiano D'amico, Valerio Acocella, Catalina Cabello, Marc Muelle Stef, Andres Tassara

PII: S0040-1951(19)30319-1

DOI: https://doi.org/10.1016/j.tecto.2019.228204

Reference: TECTO 228204

To appear in:

Received Date: 20 March 2019

Revised Date: 12 September 2019

Accepted Date: 14 September 2019

Please cite this article as: Lupi M, Trippanera D, Gonzaélez D, D'amico S, Acocella V, Cabello C, Stef MM, Tassara A, Transient tectonic regimes imposed by megathrust earthquakes and the growth of NW-trending volcanic systems in the Southern Andes, *Tectonophysics* (2019), doi: https://doi.org/10.1016/j.tecto.2019.228204

This is a PDF file of an article that has undergone enhancements after acceptance, such as the addition of a cover page and metadata, and formatting for readability, but it is not yet the definitive version of record. This version will undergo additional copyediting, typesetting and review before it is published in its final form, but we are providing this version to give early visibility of the article. Please note that, during the production process, errors may be discovered which could affect the content, and all legal disclaimers that apply to the journal pertain.

© 2019 Published by Elsevier.

Journal Pre-proof

Transient tectonic regimes imposed by megathrust earthquakes and the growth of NW-trending volcanic systems in the Southern Andes

Matteo Lupi[a], Daniele Trippanera[b,c], Diego González[d], Sebastiano D'amico[e], Valerio Acocella[b], Catalina Cabello[d], Marc Muelle Stef[d], Andres Tassara[d, f]

[a] Department of Earth Sciences, University of Geneva, Geneva, Switzerland
[b] Dipartimento di Scienze Geologiche, Università Roma Tre, Roma, Italy
[c] Department of Earth Sciences and Engineering, King Abdullah University of Science and Technology (KAUST), Thuwal, Saudi Arabia
[d] Universidad de Concepción, Departamento Ciencias de la Tierra, Concepción, Chile
[e] Department of Geosciences, University of Malta, Malta
[f] Millennium Nucleus: The Seismic Cycle along Subduction Zones, ICM-Minecom, Chile
Email address: (M. Lupi) matteo.lupi@unige.ch

Highlights

- We show the existence of a transient tectonic regime imposed by megathurust earthquakes on volcanic arc.
- The transient regime is extensional in a broadly compressive environment.
- The transient regime may be able to explain the development of NW-striking volcanic complexes in the Southern Andes.

Abstract

Geophysical data show that megathrust earthquakes can promote transient tectonic regimes lasting up to several decades. However, such variations are not trivial to be recognises in the geological records of volcanic arcs. To better understand the occurrence of transient tectonic regimes we study the inter- and post-seismic deformation in the upper crust of the Andean volcanic arc affected by the M8.8 2010 Maule earthquake. We focus on the region around the Nevados de Chillán Volcanic Complex, Southern Central Chile, where we compare geological and earthquakes data. This NW-oriented Andean-transverse volcanic complex faces one of the regions that slipped the most during the 2010 M8.8 Maule earthquake.

Field fault-slip data from lithostratigraphic units forming the basement of Nevados de Chillan Volcanic Complex point out three tectonic regimes. The principal is driven by a sub-horizontal and NE-oriented σ_1 (transpressional kinematics). This regime is compatible with today's GPS data recorded during inter-seismic periods. The second and third tectonic regimes are less abundant and indicate transpression (σ_1 sub-horizontal and NW-oriented) and normal (σ_1 sub-vertical and E-W-oriented) faulting, respectively. The geological record was also compared with seismic data acquired from 2010 to 2015 in the investigated region. The moderate-magnitude seismic activity occurred beneath the volcanic arc after the Maule earthquake points out an enhanced crustal deformation if compared to inter-seismic periods. The inversion of focal mechanisms suggests that intra-arc regions may experience a short-lived post-seismic transtensional regime with an E-W oriented σ_1 with a dip of about 45°.

Our work suggests that megathrust earthquakes impose transient stress variations in the volcanic arc, possibly reactivating Oligo-Miocene NW-striking inherited crustal structures, upon which

Journal Pre-proof

volcanic edifices develop. This may help explaining the occurrence of Andean-transverse volcanic complexes oriented sub-perpendicular to the NE-oriented σ_1 driving convergence in the Southern Andes.

Keywords: Maule earthquake, stress rotation, oblique subduction, tectonic switch, post-seismic, static stress triggering

1. Introduction

The sequence of large-magnitude megathrust earthquakes of Sumatra (2004), Chile (2010), and Japan (2011) allowed the scientific community to gather insightful information about the post-seismic tectonic deformation taking place in the upper plate of convergent plate boundaries. The geophysical community mainly focussed on post-seismic subduction and forearc tectonics (Araki et al., 2006; Lange et al., 2012; Lengliné et al., 2012; Nishimura et al., 2011; Rietbrock et al., 2012). For example, Ryder et al., (2012) described extensional faulting in the Chilean forearc after the 2010 M8.8 Maule (herein Maule) earthquake. Similar dynamics are pointed out by Imanishi et al., (2012) after the 2011 M9.0 Tohoku earthquake. Despite these two cases, only few field-oriented studies describe the tectonic deformation occurring years to decades after the main-slip in volcanic arcs affected by megathrust earthquakes (Acocella et al., 2018; Bonali, 2013, Bonali et al., 2013, 2015; Tibaldi, 2015). Moderate to large magnitude earthquakes may cause elevated dynamic and static stress in the near- and far-field activating fault systems and quiescent magmatic and mud volcanoes (e.g. Hill et al., 2002; Marzocchi, 2002; Walter and Amelung, 2007; Eggert and Walter, 2009; Lupi et al., 2013). Static and dynamic stress triggering operate at different time-scales and distances. Dynamic triggering occurs at both short and long distances and it is due to the mechanical displacement occurring at the pore scale in the geological media affected by the passing seismic waves (Hill et al., 2002; Ichihara and Brodsky, 2006). The transient strain may be induced by both body (Lupi et al., 2017a, 2013) and surface waves (Hill and Prejean, 2015; Lupi et al., 2017b). The activated geological processes may become apparent within days (Farías et al., 2014) or even years (Lupi et al., 2017a; Manga and Brodsky, 2006; Parsons, 2005; Sawi and Manga, 2018) after the main shock. Static stress triggering is broadly confined to fault rupture distances and takes place days to years after the main shock (Bonini et al., 2016; Toda et al., 2011). Static stress triggering is driven by the change in tectonic stress imposed by the seismic slip on the geological structures affected by the seismic event. Bonali et al., (2013, 2015) investigated the earthquake-induced static stress changes imposed by the Maule earthquake on volcanic systems of the Southern Central Andes. Bonali et al., (2015) showed that volcanic systems erupting after the Maule earthquake experienced unclamping or very small clamping effects (i.e. <0.5 MPa). According to Bonali et al. (2015) the Maule earthquake may promote eruptions as far as 450 km from the epicentre, and may have caused the 2012 Copahue eruption (Bonali, 2013). The Maule earthquake also caused the reactivation of seismic activity in the Andean arc via static stress variations (Spagnotto et al., 2015).

Journal Pre-proof

While static stress triggering is commonly associated to elastic processes, the seismically-induced viscoelastic relaxation of the asthenosphere can also affect the long-term post-seismic tectonic deformation in the upper plate. Hill et al., (2002) and Marzocchi, (2002) suggest that viscoelastic relaxation may cause an increase of eruptive activity in volcanic arcs. For instance, the uplift in the Central Nevada Seismic Belt is proposed to be related to the post-seismic mantle relaxation induced by a sequence of large seismic events occurred in the area from 1915 to 1954 (Gourmelen and Amelung, 2005).

In this context, one of the fundamental uncertainties in Earth Sciences is the mechanism controlling fault reactivation and kinematic changes after large magnitude earthquakes. Hardebeck and Okada, (2018) provide a comprehensive review of stress changes caused by earthquakes in trench regions. The post-seismic stress rotation for trench regions due to more recent megathrust earthquakes is discussed also by Hardebeck, (2012). For volcanic arc regions Lupi and Miller, (2014) postulated a short-lived tectonic switch taking place in the volcanic arc after megathrust earthquakes. Acocella et al., (2018) combined literature and field structural data from Sumatra pointing out a transient stress field operating during co- and post-seismic times possibly activated by megathrust earthquakes. Transient tectonic regimes may be particularly effective at oblique margins where the compressive component of the oblique subduction is reduced after the megathrust slip and the lateral component of the oblique convergence is accommodated in the arc. At oblique convergent margins the shear component may be accommodated in the overriding plate by trench-parallel, regional-scale, strike-slip faults that are localised within the volcanic arc. Several authors investigated the dynamics of such a strain partitioning using experimental (Burbidge and Braun, 2004; Pinet and Cobbold, 1992), mathematical (Platt, 1998), and field (Rosenau et al., 2006) data. Strain partitioning can create favourable conditions for magma emplacement in the arc (e.g. Rosenau et al., 2006; Sielfeld et al., 2019). However, NW-striking alignments of volcanic centres in Southern Central Chile (Figure 1) are hard to explain by strain partitioning alone (Cembrano and Lara, 2009). While the Nevados de Chillán or Cordon Caulle volcanoes (pink short lines in Figure 1) are clearly elongated NW-SE, other volcanoes (for instance Villarica - Quetrupillan - Lanin, blue lines in Figure 1) align NW-SE lying on inferred crustal-scale tectonic lineaments. Such NW-striking deep-reaching structures were suggested to be active since the development of Carboniferous-Permian basins in the Gondwana and have been suggested to be cyclically reactivated by megathrust earthquakes (Melnick et al., 2009; Stanton-Yonge et al., 2016). Sielfeld et al., (2019) provide a comprehensive list of studies that investigated such Andean-transverse systems and how they may be reactivated by earthquakes.

In order to better understand the structural control on the magmatic arc of the Southern Andes, and to further constrain any stress variation induced by the seismic cycle, we study the region around the Nevados de Chillán volcanic complex (NdCVC). This volcano is an Andean transverse NW-

Journal Pre-proof

striking complex at high-angle to the direction of subduction. We focus on the role of short-lived kinematics occurring in the years following the main-slip of the Maule earthquake trying to highlight stress tensor orientation changes at the large and at the local scale. Specifically, our working hypothesis investigates whether any tectonic change could have taken place in the volcanic arc of Southern Central Chile after major earthquakes in the past and after the Maule earthquake. The post-seismic tectonic deformation occurring in the upper crust of the South American plate is investigated by comparing post-Maule earthquake data with geological information mapped in the field. The former point out the short-term post-seismic regime and the latter the long-term inter-seismic deformation. We selected the NdCVC as it faces one of the two regions that experienced the maximum slip during the Maule earthquake (Moreno et al., 2010; Vigny et al., 2011).

The work is structured as follows: first we present results of a geological survey conducted around and within the NdCVC. This illustrates the long-term inter- and co-seismic seismic tectonic regimes that took place in the region. Next, we investigate the post-seismic regime resulting from the study of focal mechanisms obtained by inverting waveform data of shallow crustal earthquakes occurred after the Maule. We discuss the moment tensor solutions in the framework of the acquired field data and available literature. We conclude discussing a model for the evolution of NW-trending volcanic systems in the Southern Andes.

2. Geological setting

2.1 Regional setting

From about 48°S to 39°S the Southern Andes are cross-cut by the Liquiñe-Ofqui strike slip system (LOFZ) that is a right-lateral transpressional fault zone (Cembrano and Lara, 2009) extending for about 1000 km SSW-NNE (Figure 1). The morphological track of the LOFZ indicates that the strike-slip regime driving the lateral deformation seems to end at about 39°S where it transitions towards a thrust-and-fold belt (Cembrano and Lara, 2009; Figure 1).

The volcanic systems of the Southern Andes are mainly distributed along the LOFZ. However, some volcanic complexes are aligned and/or elongated along NE or NW directions (e.g. Sielfeld et al., (2019), Figure 1). Some of the NE- to ENE-striking alignments of volcanoes are associated to transtensional structures and tension cracks NE- to ENE-oriented (i.e. tail cracks, Riedel shear planes) related to the dextral kinematics of the LOFZ (Cembrano and Lara, 2009; Pérez-Flores et al., 2016). For this reason, these structures are considered kinematically compatible with the present-day convergence between the Nazca and South American plates (Cembrano and Lara, 2009; Lara et al., 2006). This is not the case for NW-elongated volcanoes (pink lines in Figure 1) or NW-trending volcanic alignments (proposed blue lines in Figure 1) striking at high-angle to the convergence

Journal Pre-proof

vector of subduction (Cembrano et al., 1996; Cembrano and Lara, 2009; Lange et al., 2008; Lavenu and Cembrano, 1999; Sielfeld et al., 2019). Compared to the volcanic systems on the LOFZ or to the NE-striking systems, NW-striking complexes show more evolved magmas (Cembrano and Lara, 2009; Bucchi et al., 2015). NW-striking structures are suggested to be controlled by NW-oriented transverse pre-Andean fault systems (Cembrano and Lara, 2009, Lara et al., 2006, Lopez-Escobar et al., 1995). However, it must be noted that NE-striking structures may be also found in NW-striking volcanic systems. This is for instance the case of the Cordon-Caulle volcano where NE-trending alignments of cones can be found both at the NE- and at the SW-end of the main volcanic edifice (Cembrano and Lara, 2009).

2.2 The 2010 M8.8 Maule earthquake

The tectonic setting of Southern Central Chile is characterised by the oblique subduction of the Nazca plate beneath the South American plate (Figure 1) at a rate of approximately 66 mm/yr (Moreno et al., 2010). This promotes megathrust earthquakes and the development of the volcanic chain about 300 km East of the trench. The most recent megathrust earthquake affecting the region is the 2010 M8.8 Maule earthquake, occurred on the 27th of February 2010 (Delouis et al., 2010; Moreno et al., 2010; Vigny et al., 2011). Early geodetic inversions (used to select the study area of this work) suggested that the earthquake ruptured at approximately 36.5°S propagating northwards until about 37.5°S and southwards until about 39° S (e.g. Delouis et al., 2010; Moreno et al., 2010). However, several finite source rupture models propose different rupture geometries (e.g. Delouis et al., 2010; Moreno et al., 2010; Vigny et al., 2011). Further information about the effects of the Maule earthquake on the volcanic arc according to the several rupture models is provided by Bonali et al., (2015). The Maule earthquake broke the Constitución (35.3°S) seismic gap (Campos et al., 2002) and stopped approximately at the Juan Fernandez Ridge to the North (Sparkes et al., 2010) and at the Mocha Fracture zone (close to the slip plane of the M9.0 1960 Valdivia earthquake) to the South (Lange et al., 2012). Lange et al., (2012) investigated the aftershock sequence of the Maule earthquake showing the tectonic deformation in the forearc from 2010 to 2012. The distribution of the aftershocks highlighted a complex setting with more crustal seismicity localised in the northern part of the rupture zone. The co-seismic GPS vectors (Delouis et al., 2010; Moreno et al., 2010; Vigny et al., 2011) indicate that the Maule earthquake imposed a maximum seaward horizontal and vertical uplift displacement in the forearc of about 5 m and 1.75 m, respectively. The volcanic arc experienced horizontal and vertical (subsidence) displacements of about 0.75 m and 0.12 m, respectively, in the region of the NdCVC. The co-seismic horizontal displacements indicated a W to WSW motion in the trench and a W to WNW motion in the arc (Delouis et al., 2010; Klein et al., 2016; Moreno et al., 2010; Vigny et al., 2011); Figure 1). InSAR data

Journal Pre-proof

also point out a post-seismic subsidence of the volcanic arc after the Maule earthquake (Pritchard et al., 2013).

2.3 Nevados de Chillán and recent eruptions

The NdCVC is located at about the northern termination of the LOFZ, in the transition zone between a marked transpressional regime (pointed out by the LOFZ) and a thrust and fold belt (e.g. Lavenu and Cembrano (1999); Cembrano and Lara, 2009). González-Vidal et al., (2018) propose that the NdCVC may sit upon the continuation of the NW-striking Cortaderas Lineament (Figure 1), in agreement with previous authors (e.g. Ramos and Kay, (2007)). The Cortaderas Lineament is a (suggested) crustal-scale discontinuity tracked in the back-arc (c.f. Hernando et al., 2012; Søager et al., 2013). This transition zone separates two regions marked by a different geological history characterised by different geometries of the subducting plate and different trench roll-back velocity (Ramos and Kay, 2007). The volcanic arc comprising the NdCVC is facing a region that was proposed to have slipped for about 10 m during the Maule earthquake (Delouis et al., 2010; Moreno et al., 2010; Vigny et al., 2011). Bonali et al., (2015) suggest that (also) NW-striking volcanic structures may have been affected by static stress changes imposed by the Maule earthquake on the volcanic arc.

The NdCVC is sub-elliptical in shape with a NW-SE oriented major axis about 16 km long and a NE-SW minor axis about 10 km long (Figure 2). The NW and SE limits of the major axis correspond to ring faults bounding an ancient caldera (Dixon et al., 1999, Naranjo, et al., 2008). The NdCVC is built upon a Cenozoic basement and consists of several emission centres aligned along a NW-SE direction (Dixon et al., 1999) (Figure 2b). The oldest geological formation of the volcanic complex is represented by sub-glacial andesitic lavas (640 ka BP) becoming sub-aerial since 100 ka BP (Dixon et al., 1999). Ignimbrites have been deposited since 40 ka BP (Naranjo, et al., 2008, Dunkley et al., 2009) when two prominent volcanic sub-complexes, the Cerro Blanco (to the NW) and the Las Termas (to the SE) began to develop on top of the ancient volcanic system (Dixon et al., 1999; Dunkley et al., 2009). The eruptive activity imposed to the NdCVC a marked ellipticity with a N140° elongation still observable (Dixon et al., 1999; Dunkley et al., 2009). Nowadays the Cerro Blanco and Las Termas are approximately 6 km apart. Over the last centuries volcanic activity focused in the SE region of the Las Termas. The most recent emission centres are named Volcan Nuevo and Arrau and formed in 1906-1945 and 1973-1986, respectively (Figure 2b; Deruelle and Deruelle, 1974; Naranjo and Lara, 2009). The three most recent eruptions of the NdCVC occurred in 2003, 2008 and late 2015 (OVDAS website; Naranjo and Lara, 2009; Coppola et al., 2016). The August-September 2003 eruption consisted of a small explosive event (VEI =0-1) that took place on the Las Termas volcanic complex between the craters Nuevo and Arrau. The explosions formed a 64 m long fissure-like double crater NW-elongated connecting the Nuevo and Arrau craters (Naranjo and

Journal Pre-proof

Lara, (2004). The 2008 eruption consisted of three small NE-oriented eruptive fissures. This small effusive eruption produced only a 0.12 km^2 lava field (Coppola et al., 2016).

The largest activity after the formation of the Arrau Volcano is the eruption that started at the end of 2015. The eruption is taking place on the summit of Las Termas complex (Figure 3). During December 2015 the seismic activity of the NdCVC remarkably increased with long period seismic events appearing along with volcano-tectonic seismicity. On the 9th of December a phreatic explosion took place at the summit of the Las Termas, on the same side of the 2003 eruption. Such a phreatic activity replicated on the 8th of January 2016. On the 9th of January aerial inspection identified a new crater to the East of the Volcan Nuevo (Figure 3a). The activity continued with the creation of three NW-SE aligned craters that finally merged into the Nicanor crater where a dome began to be extruded in 2016 (Figure 3b). For a full description of the eruptive activity we suggest to refer to Moussallam et al., (2018).

3. Methods

3.1. Geology

We conducted a geological survey around and within the NdCVC. The main goal of this part of the study was to describe the long-term tectonic deformation of the region and to understand how the local tectonics may affect/drive magmatism. During the geological surveys, we measured fault planes, dikes and eruptive fissures. Dike thickness and any relationship with the nearest faults have also been considered. To define fault kinematics we studied kinematic indicators such as mechanical striations, mineralised shear veins and smears. We used our fault data (strike, dip and rake) to perform a kinematic analysis with Faultkin software (Allmendinger et al., 2012) and dynamic analysis using MIM software (Yamaji, 2000).

The kinematic analysis allows us to understand the dominant deformation trend and the associated kinematics. The dynamic analysis investigates stress tensor configurations that may explain measured fault-slip data. The optimal stress field is parameterized by the strike and hinge of σ_1 and σ_3 and the stress ratio $\varphi=(\sigma_2-\sigma_1)/(\sigma_2-\sigma_3)$. This allows identifying stress tensor orientations that can explain the largest population of subsets. Due to difficult logistics and to the inaccessibility of certain regions, the dataset is not homogeneously distributed (i.e. the Northern sector of the NdCVC could not have been investigated). However, the entire dataset contains a large amount of data retrieved from both the area corresponding to the Nevados de Chillán edifice and the surrounding regions (Figure 2).

3.2. Seismicity

Journal Pre-proof

By using the dataset of González-Vidal et al., (2018) we inverted moment tensor solutions for earthquakes shallower than 35 km occurring beneath the volcanic arc occurred after the Maule earthquake (seismic events highlighted by grey lines in Table 1). The source depth and focal mechanisms are determined using a grid search technique based on broadband waveform inversion (Zhu and Helmberger, 1996). The method allows time shifts between synthetics and observed data in order to reduce dependence of the solution on the assumed velocity model and on earthquake locations. In order to obtain reliable source mechanisms using waveforms it was necessary to compute synthetic seismograms, which in turn requires a reasonable velocity model for generating Green's functions. We used the frequency-wavenumber (F - K) integration method described by Zhu and Rivera, (2002) to compute the Green's function and the 1-D velocity model proposed for the area (Bohm et al., 2002). We also added densities based on the Nafe - Drake relation (Nafe and Drake, 1957). The Qp and Qs values are not critically important as we are dealing with relatively short propagation distances and low frequencies. This method was already successfully applied to investigate moment tensor solutions for seismic events with M<M3.0 (Baruah and Boruah, 2018; D'Amico et al., 2010). Data were inverted to compute the confidence limits of the principal stress tensors using the method proposed by Vavryčuk, (2014).

4. Results

4.1. Structural field data

We investigate the dike directions inside and outside the Nevados de Chillán edifice (19 out of 42 dikes are located within the NdCVC, Figure 4a). This does not include the NE-oriented 2008 eruptive fissure located in the northern flank of Volcán Nuevo (Station 9 in Figure 2, Coppola et al., (2016)). A second well-documented NW-oriented eruptive fissure appeared on top of the NdCVC between the Arrau and Nuevo cones during the 2003 (eruption VEI=1) (Naranjo and Lara, 2004). Figure 3a points out that the 2015-2018 eruption also began by forming a NW-striking fissure on the side of 2003 fracture.

We classified dikes as large (≈ 2.0 m thick), medium (<2.0 m and >1.0 m thick) and small (<1.0 m thick). The thickness of the measured dikes varies from 0.5 m to 5.5 m with up to 20% of them being ≈ 2.0 m thick (Figure 4a). About 60% of the dikes strike from NE to ENE (Figures 2 and 4). More specifically, the rose diagram (Figure 4a) shows that the two main striking directions are N25°E ± 5° and N55°E ± 5°. A minor amount of dikes (≈38%) strikes from E-W to NW. In particular ≈17% of them strike N50°W ± 20°. Overall, dike directions inside and outside the edifice are consistent and show a dominating NE to ENE direction. 55% of the dikes occurring in the volcanic edifice strike N50°E ± 20° and only 25% of them strike N50°W ± 20° (Figure 4a).

Journal Pre-proof

Similarly, ≈45% of dikes outside the volcanic edifice strike N40°E ± 20° and only a minor amount strikes about N80°E ± 10° (≈25%) or N40°W ± 10° (≈12%) (Figure 4).

Figure 2b shows that large dikes strike NE (the only exception has been found in station n. 11) along with the 2003 and 2015-18 (Figure 3a) eruptive fissures striking NW. Dikes striking NW have a medium or small thickness (e.g. stations 7, 12 and 13 in Figure 2).

We measured a total of 124 faults divided into three broad groups (see Figure 4b). Note that in order to keep the description of the groups easy to follow we distinguish the three groups in terms of broad directions of the orientation of σ_1, i.e. NE-, NW-, and E-W-striking. For the precise orientation of the stress tensors, the reader is referred to Figure 5. The first and most abundant cluster consists in NE-striking structures (from N30°E to N80°E). This cluster is compatible with the current tectonic regime driving the oblique subduction. The second more abundant cluster consists in NW-striking faults (N40°W ± 20°), subparallel to the elongation of the NdCVC. The third group, although well-recognizable, counts less occurrences and it is marked by a E-W strike (N85°E and N85°W ± 5°). We collected lineations on 90 fault planes that show a prevalence of lateral kinematic ranging from less prominent to purely strike slip (mainly associated to the NE- and NW striking fault families). In particular, the NE-striking structures show dextral kinematics, while NW-striking structures show both sinistral and dextral motions. The E-W structures have a dip-slip component often prone to extension (or very prominent transtension). Figure 5a highlights the directions and dips of σ_1 and σ_3 supporting the occurrence of the three clusters mentioned above. When considering only faults found in the Quaternary volcanic deposits (i.e. the volcanic edifice), the third cluster is no longer visible (Figure 5b). However, the first (σ_1 NE-striking) and the second (σ_1 NW-striking) clusters are still found. Observations at the centimeter scale show a similar scenario where sets of veins mainly NE- and NW-striking repeatedly cross-cut each others.

NE-oriented faults are often associated with large or medium dikes intruded in the damage zones. Figure 6 shows how a well-developed NE-striking fault system (directions ranging from N50° to N60°) is characterised by the presence of a dike emplaced along the damage zone. The dike probably reached the surface feeding a lava flow (insets of Figure 6) in the uppermost part of the faulted region. The relationship between the NE-striking dike and the fault is also visible in the area to the SW of NdCVC (station 12, Figure 2).

4.2. Seismicity data

Figure 7a shows the distribution of the seismic events larger than M4.0 affecting Chile since 1975 (CMT and USGS catalogues). Geophysical data of recent megathrust earthquakes indicate that the most active post-seismic tectonic deformation induced by megathrust slips takes place within the 5 years following the main-slip (Sun et al., 2018). For this reason, we compare the crustal seismic activity 5 years before and 5 years after the Maule earthquake. To the North of the investigated

Journal Pre-proof

area, at about 34°S, pre-Maule focal mechanisms indicate extension in the volcanic arc (Figure 7a). To the South of the investigated area the deformation of the volcanic arc is dominated by strike slip faulting associated to the Liquiñe-Ofqui intra-arc fault zone. Figure 7b shows that in the arc and more specifically in the area around the NdCVC little to no seismicity occurred in the upper crust before the Maule earthquake. The only recorded events occurred below a depth of 50 km at about the subduction interface (Figure 7b). After the Maule earthquake we recorded several seismic events larger than M4.0 (see table 1) beneath the volcanic arc (Figure 7c). Part of them was shown by Lange et al., (2012) who pointed out a NW-trending distribution of the epicentres in plain view. By using the network deployed by González-Vidal et al., (2018) we calculated the focal mechanisms of earthquakes below the arc (Figure 8a). We focused on events shallower than 35 km to investigate crustal processes only. The focal mechanisms suggest complex kinematics. The fault planes of these events broadly strike either NE-SW or NW-SE with a dominant right- or left-lateral strike slip kinematic, possibly associated with an extensional component. The computation of the main stress tensors for the post-seismic period (Figure 8c) indicates that beneath the arc σ_1 is broadly E-W, σ_2 strikes NE-SW and σ_3 NW-SE. The dip of σ_1, σ_2, and σ_3 is about 45°, 50° to 75°, and 60°, respectively.

In order to understand possible changes in the orientation of the principal stress tensors before and after the Maule, we compared the stress tensor solutions from events occurred in the trench by Hardebeck, (2012) (Figure 8b) with the ones inverted in this study for the arc (Figure 8c). Hardebeck, (2012) considers six months before and six months after the Maule earthquake, as discussed in the next section.

5. Discussion

To investigate the occurrence of post-seismic short-lived tectonic regimes in volcanic arcs affected by megathrust earthquakes, we considered the orientation of the regional and local (i.e. around the NdCVC) stress fields during inter-and post-seismic times. The GPS vectors extracted from geodetic networks during inter-seismic periods indicate a NE-striking motion with interseismic GPS velocities sub-parallel to the convergence velocity (e.g. Ruegg et al., 2009, Moreno et al., 2010). GPS vectors of co-seismic and post-seismic periods indicate an E-W striking seawards motion of the overriding plate (Moreno et al., 2012, 2010; Vigny et al., 2011).

Our fault data are heterogeneous and point out the occurrence of three different clusters (Figure 4b) driven by three regimes (Figure 5). The dominant deformation is related to broadly NE-striking (strike-slip to transpressive) dextral structures. This regime is the most abundant and it is compatible with the current plate motion with a NE-oriented convergence (e.g. Ruegg et al., 2009). The second cluster is NW-striking and it seems ubiquitous in other regions (according to unpublished preliminary studies) where NW-inherited structures are present. This should be

Journal Pre-proof

further verified by targeted studies. Finally, Figure 5a shows a third cluster pointing out extensional faulting. Normal faults are sparse in the field, yet present (Figure 6b). Interestingly, the orientations of the stress tensors of this cluster are compatible with the ones inverted from the earthquakes recorded below the arc during post-seismic periods (Figure 7c) and are also compatible with the horizontal displacement vectors shown by GPS data during post-seismic periods (Vigny et al., 2011, see also Figure 1). For this reason, we speculate that cluster 3 may represent the short-lived tectonic regime imposed by megathrust earthquakes responsible for the reactivation of NW-striking inherited crustal lineaments upon which some volcanic system develops. Figure 5b shows that the third cluster cannot be recognised in the volcanic edifice. We speculate that the loose volcanic deposits, the unstable volcanic flanks and the active volcanic activity may have contributed to hide any record of extension in the edifice. This is compatible with a scenario where megathrust slip-promoted normal faulting is progressively less effective from the trench to the arc, in agreement with Nakamura and Uyeda (1980). This implies that the transient post-seismic regime may not be characterised by the same orientation of the principal stress tensors in the near- (i.e. trench) and in the far-field (volcanic arc). For instance, the orientation of the stress tensors calculated by Hardebeck et al., (2012) for the trench during inter-seismic periods (Figure 7b) shows an E-W striking quasi-horizontal σ_1 and a vertical σ_3 (Figure 7b). Although in broad agreement, this regime slightly differs from the NE-striking cluster recognised around the NdCVC (Figure 5) representative of inter-seismic periods. Similar observations may be drawn for the post-seismic period. The orientation of the principal stress tensors during the post-seismic period in the trench (Hardebeck, 2012) shows an E-W striking σ_1 with a dip (that underwent a vertical rotation) of about 30° (σ_3 strikes E-W and has a dip of about 45°). The strike of σ_1 in the volcanic arc inverted from aftershock earthquakes (Figure 7c) and from field data (Figure 5a) is in agreement with the E-W direction of σ_1 in the trench shown by Hardebeck (2012) for the post-seismic period. The dip of σ_1 becomes progressively more vertical from the trench (Figure 7c) to the volcanic arc (Figure 5b). The orientation of σ_3 is complex to explain (and we refrain from doing so), as it may be affected by the local regime.

In this tectonic setting the NW-elongation of the Nevados de Chillán, requires some further discussion. Radic, (2006) proposes that the NW-striking elongation of the NdCVC is compatible with a structural setting where the Nevados de Chillán develops upon an accommodation structure between two extensional Oligo-Miocene basins (Cuenca Chillán and Cuenca Lileo). The two basins are separated by a NW-striking shear zone that may have caused the focusing of volcanism. Lavenu and Cembrano, (1999) and Cembrano and Lara, (2009) propose that the NdCVC develops upon an inherited Oligo-Miocene NW-striking crustal discontinuity and that fluids at supra-lithostatic pressure may reactivate such a lineament. We agree on the importance of inherited crustal-scale structures in controlling the development of Andean-transverse volcanic complexes, and in

Journal Pre-proof

particular the growth of the NdCVC. Indeed, the shear wave tomography around the NdCVC (extracted from González-Vidal et al., 2018) suggests the presence of a broad region of lower shear wave velocities striking NW-SE, subparallel to the elongation of the NdCVC (Figure 9). It is well-established that the velocity of shear waves is reduced in highly fractured regions and it is sensitive to the occurrence of fluids. We propose that the NW-striking anomaly shown in Figure 9 may be linked to crustal discontinuities (e.g. the Cortaderas Lineament, Ramos and Kay, 2007) and/or to the accumulation of fluids (e.g. magmas or fluids upwelling from the dehydrating slab; see also González-Vidal et al., 2018) in agreement with Cembrano and Lara (2009).

In the inter-seismic stress field characterised by a NE-trending σ_1 (Delouis et al., 2010; Moreno et al., 2010; Radic, 2006; Vigny et al., 2011) NW-SE oriented volcanic alignments should be locked and in a compressional regime, which in turn would hinder the upwelling of magmas. The NW-striking structures proposed to occur in Southern Central Chile (blue lines in Figure 1) are also not in agreement with Nakamura et al., (1977) who suggest that the distribution of volcanoes and their elongation is subparallel to σ_1. However, Nakamura et al., (1977) draw general observations not considering additional factors such as inherited deep structures and the perturbing effects that megathrust earthquakes may impose on such crustal lineaments. The reactivation of crustal NW-striking Andean transverse fault systems during post-seismic periods may be explained by the sub-vertical dip of σ_1 pointed out by normal faults, which implies extension. The agreement of the strike of σ_1 retrieved from field structural data with geophysical data (seismic and GPS) further supports an extensional environment where the upwelling of fluids (e.g. magmas) at supra-lithostatic pressure is promoted (Cembrano and Lara, 2009; Tibaldi, 2005).

To understand how NW-striking dike emplacements and volcanism may take place in the Andean Cordillera of Southern Central Chile it is important (in our opinion) not to consider the chain build up like a steady process, driven by a steady tectonic regime. The Chilean margin is recurrently shaken by violent megathrust earthquakes that may impose an acceleration of otherwise steady geological processes. These events not only may enhance the production and upwelling of deep fluids and magmas resulting into an increase of the volcanic activity (e.g. Hill et al., 2002 and Walter and Amelung, 2006), but may also promote the occurrence of short-lived tectonic regimes by re-orienting the principal stress tensors.

Volcanic unrest promoted by earthquakes is often associated with static stress triggering. This mechanism postulates a variation of the local stress field imposed by an earthquake on a given receiving fault/structure. Our proposed corollary is that such stress changes are due to a short-lived new local stress field where the orientation of the stress tensors may be rotated with respect to the inter-seismic period.. This transient regime may fade-away within years to decades when the long-term regional regime will be recovered. Bonali et al., (2015) show that the Maule earthquake did affect the Nevados de Chillán by imposing post-seismic normal stress perturbations ranging

Journal Pre-proof

from 0.1 MPa to 0.5 MPa on NW striking and NE-striking receiver faults, respectively. Spagnotto et al., (2015) pointed out that such an unclamping may have temporarily changed the local regime from compressional to transtensional (or in some cases extensional) causing the reactivation of Quaternary faults. Our data point out that after the Maule earthquake moderate magnitude events (Table 1) occurred beneath the volcanic arc (Figure 7c), where no seismic activity occurred in the years preceding the megathrust event (Figure 7b).

Figure 10 summarises the processes that we suggest may occur before and after the Maule earthquake in the investigated region. During inter-seismic periods (Figure 10a) the trench is characterised by an orientation of the principal stress tensors typical of compressional environments (Figure 8b, Hardebeck 2012). NE-striking dikes, driven by the regional stress field may feed the deep main sill-like reservoir (Tibaldi, 2015) of the NdCVC, which is suggested to be located in a ramp-and-flat structure along an inherited NW-oriented fault as proposed by Cembrano and Lara (2009) and Sanchez et al., (2013) for other volcanic systems of the Southern Andes. This is supported by field data showing several evidences of dikes intruding (or are close to, i.e. <5 m) NE-striking faults. The agreement between fault and dike directions is particularly evident further away from the central edifice of the NdCVC (e.g. stations 8 and 12; Figure 2), where magma intruding along NE-directions seems to be driven by the inter-seismic regional regime (Cembrano and Lara, 2009; Lavenu and Cembrano, 1999; Pérez-Flores et al., 2016). During inter-seismic periods pre-existing NW-striking structures are locked and fluid (or magma) flow is possibly hindered.

During and after the megathrust slip the upper plate is unloaded and the local kinematics become complex and not trivial to constrain (Figure 10b). The inversion of field and earthquake data, in agreement with GPS records, suggests the occurrence of an E-W striking extension driven by the megathrust slip. Below the volcanic arc σ_1 becomes subvertical promoting the upwelling of deep magmas. We observe that deformation taking place in the trench differs from the one taking place below the arc and from the one taking place at the surface. In the months following the megathrust slip the compression initially reduced (i.e. the magnitude of σ_1) of up to about 80% (Hardebeck, 2012) is rapidly recovered in the trench. However, extension in the upper crust continues as shown by seismic (Ryder et al., 2012) and GPS data (Klein et al., 2016). The maximum slip and the horizontal and vertical displacements progressively decrease towards the surface (Moreno et al., 2010, Klein et al., 2016). Vice-versa, locking propagates from the subduction interface upwards. This may facilitate the unzipping of crustal-scale structures along which fluids at supra-lithostatic pressure released from the dehydrating slab and deep magmas may intrude. Such mechanism may be enhanced below the arc where the more vertical dip of σ_1 suggests extension (Figure 5) and/or transtension (Figure 8c). Indeed, the inversion of the focal mechanisms point out that below the arc

Journal Pre-proof

σ_1 rotates its dip to about 45° while maintaining a E-W-strike orientation (Figures 8c, and 10b) and σ_3 rotates to sub-horizontal (30°) promoting a broadly extensional environment at depth. In this context, the Oligo-Miocene lineaments upon which the NdCVC resides (Cembrano and Lara, 2009; González-Vidal et al., 2018) may be reactivated and pervaded by deep fluids. We propose that such processes may also have been occurring in other regions of the Southern Central Andes, where NW-striking alignments of volcanic edifices are found. For instance, the prolonged extension at the surface pointed out by GPS data (Wang et al., 2002) was postulated for the reactivation of the NW-striking Cordon-Caulle volcanic system after the M9.5 1960 Vadilvia earthquake (Lara et al., 2006; Plafker and Savage, 1970).

Our proposed mechanism is certainly not definitive, as we cannot rely on stress tensor distributions derived from focal mechanisms below the volcanic arc before the Maule earthquake. However, we point out the complexity of the tectonic processes taking place in the arc after megathrust earthquakes and describe how such mechanisms may drive the reactivation of NW-striking volcanic systems favouring the development of Andean transverse volcanic systems.

6. Conclusions

Field evidence of megathrust-driven tectonic inversions may be hidden in the geological records. However, geophysical data have shown that short-lived mechanisms may take place in the upper plate of convergent margins after megathrust earthquakes. We compared geological records and seismic data to investigate the occurrence of transient tectonic regimes taking place in the volcanic arc of the Southern Central Chile after the M8.8 Maule earthquake.

The structural field data show three different tectonic regimes. The first two regimes are compatible with GPS data recorded during inter-seismic periods and support NE-oriented and NW-oriented σ_1 compatible with a transpressional regime. The third regime shows an E-W striking σ_1 with subvertical dip below the volcanic arc. We speculate that this regime may represent a transient stress state imposed by the megathrust slip that may promote the upwelling of magmas from depth. These data are in agreement with inverted focal mechanisms retrieved from moderate-magnitude seismic events occurred below the volcanic arc after the Maule earthquake. The seismic activity also point out that in the 5 years following the Maule earthquake the crustal deformation was enhanced beneath the volcanic arc.

Our study highlights that geological processes taking place in volcanic arcs of compressional margins are not steady, but can be characterised by periods of accelerated and changed deformation promoted by megathrust earthquakes. We point out that the evolution of NW-striking systems in Southern Central Chile is complex and requires further investigations where the role of megathrust earthquakes is scrutinised further.

Journal Pre-proof

Acknowledgments

The authors thanks Cristian, Luis, and Macarena for their help while in Chile. The Seismological service of Chile and OVDAS are acknowledged for the seismic data. We thank the GIPP (Geophysical Instrument Pool Potsdam), Germany, for providing the instruments for the experiment of Gonzalez et al., (2018). The facilities of IRIS Data Management Centre were used for accessing the waveforms and related metadata used in this study. Matteo Lupi thanks SCCER-SoE and the Swiss National Science Foundation for financial support (grant NPZ00P2_154815 and PYAPP2_166900). Prof. Alessandro Tibaldi and an anonymous Reviewer reviewed this manuscript remarkably contributing to improve the study. The seismic data are stored on GFZ servers and can be requested here: https://gipp.gfz-potsdam.de/webapp/projects/view/248

REFERENCES

Acocella, V., Bellier, O., Sandri, L., Sébrier, M., Pramumijoyo, S., 2018. Weak Tectono-Magmatic Relationships along an Obliquely Convergent Plate Boundary: Sumatra, Indonesia. Front. Earth Sci. 6, 3. doi:10.3389/feart.2018.00003

Acocella, V., Tibaldi, A., 2005. Dike propagation driven by volcano collapse: A general model tested at Stromboli, Italy. Geophys. Res. Lett. doi:10.1029/2004GL022248

Allmendinger, R. W., Cardozo, N. C., and Fisher, D., 2012, Structural Geology Algorithms: Vectors & Tensors: Cambridge, England, Cambridge University Press, 289 pp.

Araki, E., Shinohara, M., Obana, K., Yamada, T., Kaneda, Y., Kanazawa, T., Suyehiro, K., 2006. Aftershock distribution of the 26 December 2004 Sumatra-Andaman earthquake from ocean bottom seismographic observation. Earth, Planets Sp. *58*(2), 113-119. doi:10.1186/BF03353367

Baruah, S., Boruah, M., 2018. Waveform Modelling of 2009 Bhutan Earthquake of Magnitude 6.1 (Mw) Using Local Network Data of North East India. Springer, Cham, pp. 389–404. doi:10.1007/978-3-319-77359-9_18

Bonali, F. L., 2013. Earthquake-induced static stress change on magma pathway in promoting the 2012 Copahue eruption. Tectonophysics, 608, 127-137.

Bonali, F.L., Tibaldi, A. and Corazzato, C., 2015. Sensitivity analysis of earthquake-induced static stress changes on volcanoes: the 2010 M w 8.8 Chile earthquake. Geophysical Journal International, 201(3), pp.1868-1890.

Bonali, F. L., A. Tibaldi, C. Corazzato, D. R. Tormey, and L. E. Lara. "Quantifying the effect of large earthquakes in promoting eruptions due to stress changes on magma pathway: the Chile case." Tectonophysics 583 (2013): 54-67.

Bonini, Marco, Maxwell L. Rudolph, and Michael Manga. "Long-and short-term triggering and modulation of mud volcano eruptions by earthquakes." *Tectonophysics* 672 (2016): 190-211.

Bucchi, F., Lara, L.E., Gutierrez, F., 2015. The Carrán–Los Venados volcanic field and its relationship with coeval and nearby polygenetic volcanism in an intra-arc setting. Journal of Volcanology and Geothermal Research, 308, 70-81

Burbidge, D.R., Braun, J., 2004. Analogue models of obliquely convergent continental plate

Journal Pre-proof

boundaries. J. Geophys. Res. Solid Earth. doi:10.1029/98jb00751

Campos, J., D. Hatzfeld, R. Madariaga, G. Lopez, E. Kausel, A. Zollo, G. Iannacone, R. Fromm, S. Barrientos, and H. Lyon-Caen. "A seismological study of the 1835 seismic gap in south-central Chile." *Physics of the Earth and Planetary Interiors* 132, no. 1-3 (2002): 177-195.

Cembrano, J., Hervé, F., Lavenu, A., 1996. The Liquiñe Ofqui fault zone: a long-lived intra-arc fault system in southern Chile. Tectonophysics 259, 55–66. doi:10.1016/0040-1951(95)00066-6

Cembrano, J., & Lara, L. (2009). The link between volcanism and tectonics in the southern volcanic zone of the Chilean Andes: a review. *Tectonophysics*, *471*(1-2), 96-113.

Coppola, D., Laiolo, M., Lara, L.E., Cigolini, C., Orozco, G., 2016. The 2008 "silent" eruption of Nevados de Chillán (Chile) detected from space: Effusive rates and trends from the MIROVA system. J. Volcanol. Geotherm. Res. 327, 322–329. doi:10.1016/J.JVOLGEORES.2016.08.016

D'Amico, S., Orecchio, B., Presti, D., Zhu, L., Herrmann, R.B., Neri, G., 2010. Broadband waveform inversion of moderate earthquakes in the Messina Straits, southern Italy. Phys. Earth Planet. Inter. 179, 97–106. doi:10.1016/J.PEPI.2010.01.012

Delouis, B., Nocquet, J.M., Vallée, M., 2010. Slip distribution of the February 27, 2010 Mw = 8.8 Maule Earthquake, central Chile, from static and high-rate GPS, InSAR, and broadband teleseismic data. Geophys. Res. Lett. doi:10.1029/2010GL043899

Deruelle, Benjamin, Deruelle, J., 1974. Estudios geológicos., in: Estudios Geológicos, ISSN 0367-0449, Vol. 30, Nº 2-3, 1974, Págs. 97-108.

Dixon, H., Murphy, M., Sparks, S., Chávez, R., Naranjo, J., Dunkley, P., Young, S., Gilbert, J., Pringle, M., 1999. The Geology of Nevados de Chillan Volcano, Chile. Rev. Geológica Chile.

Dunkley, P.N., Sparks, S.J., Pringle, M.R., Young, S.R., Murphy, M.D., Naranjo, J.A., Dixon, H.J., Chávez, R., Gilbert, J.S., 2009. The geology of Nevados de Chillán volcano, Chile. Rev. Geológica Chile. doi:10.4067/s0716-02081999000200006

Eggert, S. and Walter, T.R., 2009. Volcanic activity before and after large tectonic earthquakes: observations and statistical significance. *Tectonophysics*, *471*(1-2), pp.14-26.

Farías, C., Lupi, M., Fuchs, F., Miller, S.A., 2014. Seismic activity of the Nevados de Chillán volcanic complex after the 2010 Mw8.8 Maule, Chile, earthquake. J. Volcanol. Geotherm. Res. 283. doi:10.1016/j.jvolgeores.2014.06.013

González-Vidal, D., Obermann, A., Tassara, A., Bataille, K., Lupi, M., 2018. Crustal model of the Southern Central Andes derived from ambient seismic noise Rayleigh-wave tomography. Tectonophysics 744, 215–226. doi:10.1016/J.TECTO.2018.07.004

Gourmelen, N., Amelung, F., 2005. Geophysics: Postseismic mantle relaxation in the Central Nevada Seismic Belt. Science (80.). doi:10.1126/science.1119798

Hardebeck, J.L., 2012. Coseismic and postseismic stress rotations due to great subduction zone earthquakes. Geophys. Res. Lett. 39, n/a-n/a. doi:10.1029/2012GL053438

Journal Pre-proof

Hardebeck, J.L., Okada, T., 2018. Temporal Stress Changes Caused by Earthquakes: A Review. J. Geophys. Res. Solid Earth 123, 1350–1365. doi:10.1002/2017JB014617

Hernando, I.R., Llambias, E.J., Gonzalez, P.D., Sato, K., 2012. Volcanic stratigraphy and evidence of magma mixing in the Quaternary Payun Matru volcano, andean backarc in western Argentina. Andean Geol. 39, 158–179. doi:10.5027/andgeoV39N1-a08

Hill, D. P., Pollitz, F., & Newhall, C. (2002). Earthquake-volcano interactions. *Physics Today*, *55*(11), 41-47.

Hill, D.P., Prejean, S.G., 2015. Dynamic Triggering, in: Treatise on Geophysics: Second Edition. doi:10.1016/B978-0-444-53802-4.00078-6

Ichihara, M., Brodsky, E.E., 2006. A limit on the effect of rectified diffusion in volcanic systems. Geophys. Res. Lett. doi:10.1029/2005GL024753

Imanishi, K., Ando, R., Kuwahara, Y., 2012. Unusual shallow normal-faulting earthquake sequence in compressional northeast Japan activated after the 2011 off the Pacific coast of Tohoku earthquake. Geophys. Res. Lett. doi:10.1029/2012GL051491

Klein, E., L. Fleitout, C. Vigny, and J. D. Garaud. "Afterslip and viscoelastic relaxation model inferred from the large-scale post-seismic deformation following the 2010 M w 8.8 Maule earthquake (Chile)." *Geophysical Journal International* 205, no. 3 (2016): 1455-1472.

Lange, D., Cembrano, J., Rietbrock, A., Haberland, C., Dahm, T., Bataille, K., 2008. First seismic record for intra-arc strike-slip tectonics along the Liquiñe-Ofqui fault zone at the obliquely convergent plate margin of the southern Andes. Tectonophysics 455, 14–24. doi:10.1016/J.TECTO.2008.04.014

Lange, D., Tilmann, F., Barrientos, S.E., Contreras-Reyes, E., Methe, P., Moreno, M., Heit, B., Agurto, H., Bernard, P., Vilotte, J.P. and Beck, S., 2012. Aftershock seismicity of the 27 February 2010 Mw 8.8 Maule earthquake rupture zone. *Earth and Planetary Science Letters*, *317*, pp.413-425.

Lara, L.E., Lavenu, A., Cembrano, J., Rodríguez, C., 2006. Structural controls of volcanism in transversal chains: Resheared faults and neotectonics in the Cordón Caulle–Puyehue area (40.5°S), Southern Andes. J. Volcanol. Geotherm. Res. 158, 70–86. doi:10.1016/J.JVOLGEORES.2006.04.017

Lavenu, A., Cembrano, J., 1999. Compressional- and transpressional-stress pattern for Pliocene and Quaternary brittle deformation in fore arc and intra-arc zones (Andes of Central and Southern Chile). J. Struct. Geol. 21, 1669–1691. doi:10.1016/S0191-8141(99)00111-X

Lengliné, O., Enescu, B., Peng, Z., Shiomi, K., 2012. Decay and expansion of the early aftershock activity following the 2011, Mw9.0 Tohoku earthquake. Geophys. Res. Lett. doi:10.1029/2012GL052797

Lopez-Escobar, L., Cembrano, J., Moreno, H., 1995. Geochemistry and tectonics of the Chilean Southern Andes basaltic Quaternary volcanism (37-46°S). Andean Geol. 22, 219–234.

Journal Pre-proof

doi:10.5027/andgeov22n2-a06

Lupi, M., Frehner, M., Weis, P., Skelton, A., Saenger, E.H., Tisato, N., Geiger, S., Chiodini, G., Driesner, T., 2017a. Regional earthquakes followed by delayed ground uplifts at Campi Flegrei Caldera, Italy: Arguments for a causal link. Earth Planet. Sci. Lett. 474. doi:10.1016/j.epsl.2017.07.006

Lupi, M., Fuchs, F., Saenger, E.H., 2017b. Numerical simulations of passing seismic waves at the Larderello-Travale Geothermal Field, Italy. Geophys. Res. Lett. 44. doi:10.1002/2016GL072417

Lupi, M., and S. A. Miller. "Short-lived tectonic switch mechanism for long-term pulses of volcanic activity after mega-thrust earthquakes." *Solid Earth* 5.1 (2014): 13.

Lupi, M., Saenger, E.H., Fuchs, F., Miller, S.A., 2013. Lusi mud eruption triggered by geometric focusing of seismic waves. Nat. Geosci. 6. doi:10.1038/ngeo1884

Manga, Michael, and Emily Brodsky. "Seismic triggering of eruptions in the far field: Volcanoes and geysers." *Annu. Rev. Earth Planet. Sci* 34 (2006): 263-291.

Marzocchi, W., 2002. Remote seismic influence on large explosive eruptions. J. Geophys. Res. Solid Earth 107, EPM 6-1-EPM 6-7. doi:10.1029/2001JB000307

Melnick, D., Bookhagen, B., Strecker, M.R., Echtler, H.P., 2009. Segmentation of megathrust rupture zones from fore-arc deformation patterns over hundreds to millions of years, Arauco peninsula, Chile. J. Geophys. Res. Solid Earth 114. doi:10.1029/2008JB005788

Moreno, M., Daniel Melnick, M. Rosenau, J. Baez, Jan Klotz, Onno Oncken, Andres Tassara et al. Toward understanding tectonic control on the Mw 8.8 2010 Maule Chile earthquake. *Earth and Planetary Science Letters* 321 (2012): 152-165.

Moreno, M., Rosenau, M. and Oncken, O., 2010. 2010 Maule earthquake slip correlates with pre-seismic locking of Andean subduction zone. *Nature*, *467*(7312), p.198.

Moussallam, Y., Bani, P., Schipper, C.I., Cardona, C., Franco, L., Barnie, T., Amigo, Á., Curtis, A., Peters, N., Aiuppa, A., Giudice, G., Oppenheimer, C., 2018. Unrest at the Nevados de Chillán volcanic complex: a failed or yet to unfold magmatic eruption? Volcanica 1, 19–32. doi:10.30909/vol.01.01.1932

Nafe, J.E., Drake, C.L., 1957. Variation with depth in shallow and deep water marine sediments of porosity, density and the velocities of compressional and shear waves. Geophysics 22, 523–552. doi:10.1190/1.1438386

Nakamura, K., Jacob, K.H., Davies, J.N., 1977. Volcanoes as possible indicators of tectonic stress orientation - Aleutians and Alaska. Pure Appl. Geophys. PAGEOPH. doi:10.1007/BF01637099

Nakamura, K., Uyeda, S., 1980. Stress gradient in arc-back arc regions and plate subduction. J. Geophys. Res. Solid Earth 85 (B11), 6419-6428

Naranjo, J.A., Jennie Gilbert, S., Stephen, R., Sparks, J., 2008. Geología del Complejo Volcánico Nevados de Chillán, Región del Biobío.

Journal Pre-proof

Journal Pre-proof

Naranjo, J.A., Lara, L.E., 2009. August-September 2003 small vulcanian eruption at the Nevados de Chillán Volcanic Complex (36°50'S), Southern Andes (Chile). Rev. geológica Chile. doi:10.4067/s0716-02082004000200011

Naranjo, J.A., Lara, L.E., 2004. August-September 2003 small vulcanian eruption at the Nevados de Chillán Volcanic Complex (36°50'S), Southern Andes (Chile). Rev. geológica Chile 31, 359–366. doi:10.4067/S0716-02082004000200011

Nishimura, T., Munekane, H., & Yarai, H. (2011). The 2011 off the Pacific coast of Tohoku Earthquake and its aftershocks observed by GEONET. *Earth, planets and space*, *63*(7), 22.

OVDAS, n.d. Red Nacional de Vigilancia Volcánica – SERNAGEOMIN URL https://www.sernageomin.cl/red-nacional-de-vigilancia-volcanica/ (accessed 3.18.19).

Kirker, A. I., & Platt, J. P. (1998). Unidirectional slip vectors in the western Betic Cordillera: implications for the formation of the Gibraltar arc. *Journal of the Geological Society*, *155*(1), 193-207.

Parsons, Tom. "A hypothesis for delayed dynamic earthquake triggering." *Geophysical Research Letters* 32.4 (2005).

Pérez-Flores, P., Cembrano, J., Sánchez-Alfaro, P., Veloso, E., Arancibia, G., Roquer, T., 2016. Tectonics, magmatism and paleo-fluid distribution in a strike-slip setting: Insights from the northern termination of the Liquiñe–Ofqui fault System, Chile. Tectonophysics 680, 192–210. doi:10.1016/J.TECTO.2016.05.016

Pinet, N., Cobbold, P.R., 1992. Experimental insights into the partitioning of motion within zones of oblique subduction. Tectonophysics. doi:10.1016/0040-1951(92)90388-M

Plafker, G., Savage, J.C., 1970. Mechanism of the Chilean earthquakes of May 21 and 22, 1960. Bull. Geol. Soc. Am. doi:10.1130/0016-7606(1970)81[1001:MOTCEO]2.0.CO;2

Radic, J.P., 2010. Las cuencas cenozoicas y su control en el volcanismo de los Complejos Nevados de Chillan y Copahue-Callaqui (Andes del Sur, 36-39°S). Andean Geol. 37, 220–246. doi:10.4067/S0718-71062010000100009

Radic, J.P., 2006. Anisotropias de basamento como control estructural del volcanismo en el complejo volcanico Chillan (Andes del Sur 36°S), in: XI Congreso Geologico Chileno, Antofagasta. p. Actas, Vol. 2, Geodinamica Andina.

Ramos, V.A., Kay, S.M., 2007. Overview of the tectonic evolution of the southern Central Andes of Mendoza and Neuquén (35°–39°S latitude), in: Special Paper 407: Evolution of an Andean Margin: A Tectonic and Magmatic View from the Andes to the Neuquén Basin (35°-39°S Lat). doi:10.1130/2006.2407(01)

Rietbrock, A., Ryder, I., Hayes, G., Haberland, C., Comte, D., Roecker, S. and Lyon-Caen, H., 2012. Aftershock seismicity of the 2010 Maule Mw= 8.8, Chile, earthquake: Correlation between co-seismic slip models and aftershock distribution?. *Geophysical Research Letters*, *39*(8).

Journal Pre-proof

Journal Pre-proof

Rosenau, M., Melnick, D. and Echtler, H., 2006. Kinematic constraints on intra-arc shear and strain partitioning in the southern Andes between 38 S and 42 S latitude. *Tectonics*, *25*(4).

Ruegg, J.C., Rudloff, A., Vigny, C., Madariaga, R., de Chabalier, J.B., Kausel, E., Barrientos, S., Dimitrov, D., 2009. Interseismic strain accumulation measured by GPS in the seismic gap between Constitución and Concepción in Chile. Phys. Earth Planet. Inter. 175, 78–85. doi:10.1016/J.PEPI.2008.02.015

Ryder, I., Rietbrock, A., Kelson, K., Bürgmann, R., Floyd, M., Socquet, A., ... & Carrizo, D. (2012). Large extensional aftershocks in the continental forearc triggered by the 2010 Maule earthquake, Chile. *Geophysical Journal International*, *188*(3), 879-890.

Sánchez, P., Pérez-Flores, P., Arancibia, G., Cembrano, J. and Reich, M., 2013. Crustal deformation effects on the chemical evolution of geothermal systems: the intra-arc Liquiñe–Ofqui fault system, Southern Andes. *International Geology Review*, *55*(11), pp.1384-1400.

Sawi, T.M. and Manga, M., 2018. Revisiting short-term earthquake triggered volcanism. *Bulletin of Volcanology*, *80*(7), p.57.

Sielfeld, G., Lange, D. and Cembrano, J., 2019. Intra-Arc Crustal Seismicity: Seismotectonic Implications for the Southern Andes Volcanic Zone, Chile. *Tectonics*, *38*(2), pp.552-578.
doi:10.1029/2018tc004985

Søager, N., Holm, P.M., Llambías, E.J., 2013. Payenia volcanic province, southern Mendoza, Argentina: OIB mantle upwelling in a backarc environment. Chem. Geol. 349–350, 36–53. doi:10.1016/J.CHEMGEO.2013.04.007

Spagnotto, S., Triep, E., Giambiagi, L. and Lupari, M., 2015. Triggered seismicity in the Andean arc region via static stress variation by the Mw= 8.8, February 27, 2010, Maule Earthquake. *Journal of South American Earth Sciences*, *63*, pp.36-47.

Sparkes, R., Tilmann, F., Hovius, N., Hillier, J., 2010. Subducted seafloor relief stops rupture in South American great earthquakes: Implications for rupture behaviour in the 2010 Maule, Chile earthquake. Earth Planet. Sci. Lett. doi:10.1016/j.epsl.2010.07.029

Stanton-Yonge, A., Griffith, W.A., Cembrano, J., St. Julien, R., Iturrieta, P., 2016. Tectonic role of margin-parallel and margin-transverse faults during oblique subduction in the Southern Volcanic Zone of the Andes: Insights from Boundary Element Modeling. Tectonics 35, 1990–2013. doi:10.1002/2016TC004226

Sun, T., Wang, K., He, J., 2018. Crustal Deformation Following Great Subduction Earthquakes Controlled by Earthquake Size and Mantle Rheology. J. Geophys. Res. Solid Earth 123, 5323–5345. doi:10.1029/2017JB015242

Tibaldi, A., 2005. Volcanism in compressional tectonic settings: Is it possible? *Geophysical Research Letters*, *32*(6), doi:10.1029/2004GL021798.

Tibaldi, A., 2015. Structure of volcano plumbing systems: A review of multi-parametric effects. J.

Journal Pre-proof

Volcanol. Geotherm. Res. 298, 85-135. doi:10.1016/j.jvolgeores.2015.03.023

Toda, S., Lin, J. and Stein, R.S., 2011. Using the 2011 M w 9.0 off the Pacific coast of Tohoku Earthquake to test the Coulomb stress triggering hypothesis and to calculate faults brought closer to failure. *Earth, planets and space*, *63*(7), p.39.

Vavryčuk, V., 2014. Iterative joint inversion for stress and fault orientations from focal mechanisms. Geophys. J. Int. 199, 69–77. doi:10.1093/gji/ggu224

Vigny, C., Socquet, A., Peyrat, S., Ruegg, J.C., Métois, M., Madariaga, R., Morvan, S., Lancieri, M., Lacassin, R., Campos, J., Carrizo, D., Bejar-Pizarro, M., Barrientos, S., Armijo, R., Aranda, C., Valderas-Bermejo, M.C., Ortega, I., Bondoux, F., Baize, S., Lyon-Caen, H., Pavez, A., Vilotte, J.P., Bevis, M., Brooks, B., Smalley, R., Parra, H., Baez, J.C., Blanco, M., Cimbaro, S., Kendrick, E., 2011. The 2010 Mw 8.8 Maule megathrust earthquake of Central Chile, monitored by GPS. Science (80-.). doi:10.1126/science.1204132

Walter, T. R., & Amelung, F. (2007). Volcanic eruptions following M≥ 9 megathrust earthquakes: Implications for the Sumatra-Andaman volcanoes. *Geology*, *35*(6), 539-542.

Walter, T.R. and Amelung, F., 2006. Volcano-earthquake interaction at Mauna Loa volcano, Hawaii. *Journal of Geophysical Research: Solid Earth*, *111*(B5).

Wang, K., Hu, Y., Klotz, J., He, J., Khazaradze, G., 2002. Prolonged post-seismic deformation of the 1960 great Chile earthquake and implications for mantle rheology. Geophys. Res. Lett. doi:10.1029/2002gl015986

Yamaji, A., 2000. The multiple inverse method: a new technique to separate stresses from heterogeneous fault-slip data. *Journal of Structural Geology*, *22*(4), pp.441-452.

Zhu, L. and Helmberger, D.V., 1996. Advancement in source estimation techniques using broadband regional seismograms. *Bulletin of the Seismological Society of America*, *86*(5), pp.1634-1641.

Zhu, L. and Rivera, L.A., 2002. A note on the dynamic and static displacements from a point source in multilayered media. *Geophysical Journal International*, *148*(3), pp.619-627.

Journal Pre-proof

Journal Pre-proof

FIGURES

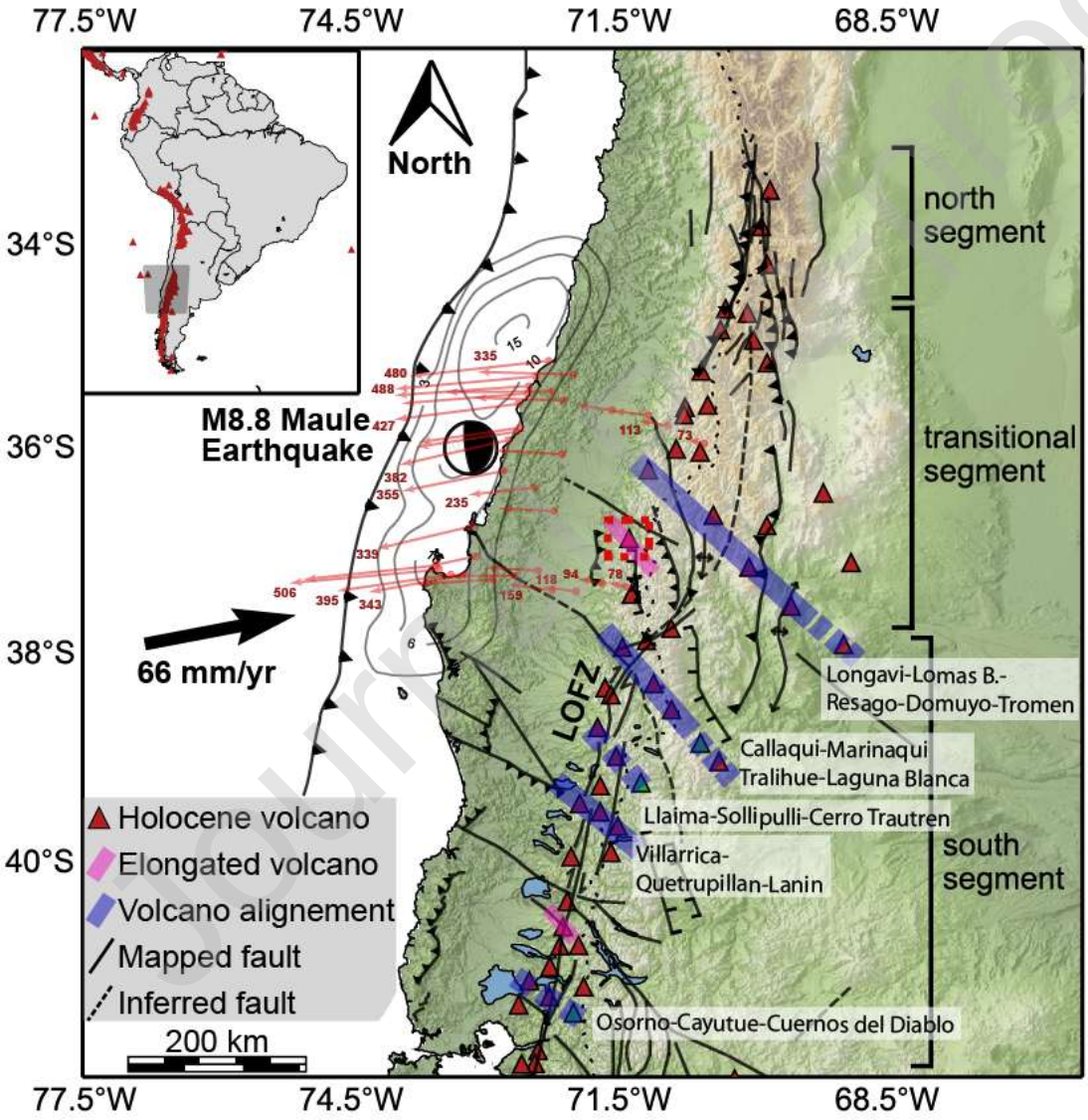

FIGURE 1

Journal Pre-proof

Simplified tectonic map of Southern Central Chile. Blue and pink bands point out suggested alignments of volcanic systems and NW-elongated volcanic centres, respectively. The distribution of the volcanic centres and the tectonic structures are taken from Gonzalez et al., (2018). Reverse, normal and strike slip faults are shown with triangles, segments, and simple black lines, respectively. The large arrow refers to the relative motion between the two plates (considering South America fixed). The orientation and rate of the convergence is N78° and 66 mm/yr (Moreno et al., 2010). The square points out the region investigated in this study. The red arrows extracted from Vigny et al., (2011) show the horizontal displacements imposed by the Maule earthquake and the red number represents the displacement in cm. The position of the NdCVC is marked by the position of the pink triangle borded by the red dashed square. North, transitional and south segment refer to the general partition of the tectonics characterising the Southern Central Andes. LOFZ stands for Liquine-Ofqui Fault Zone.

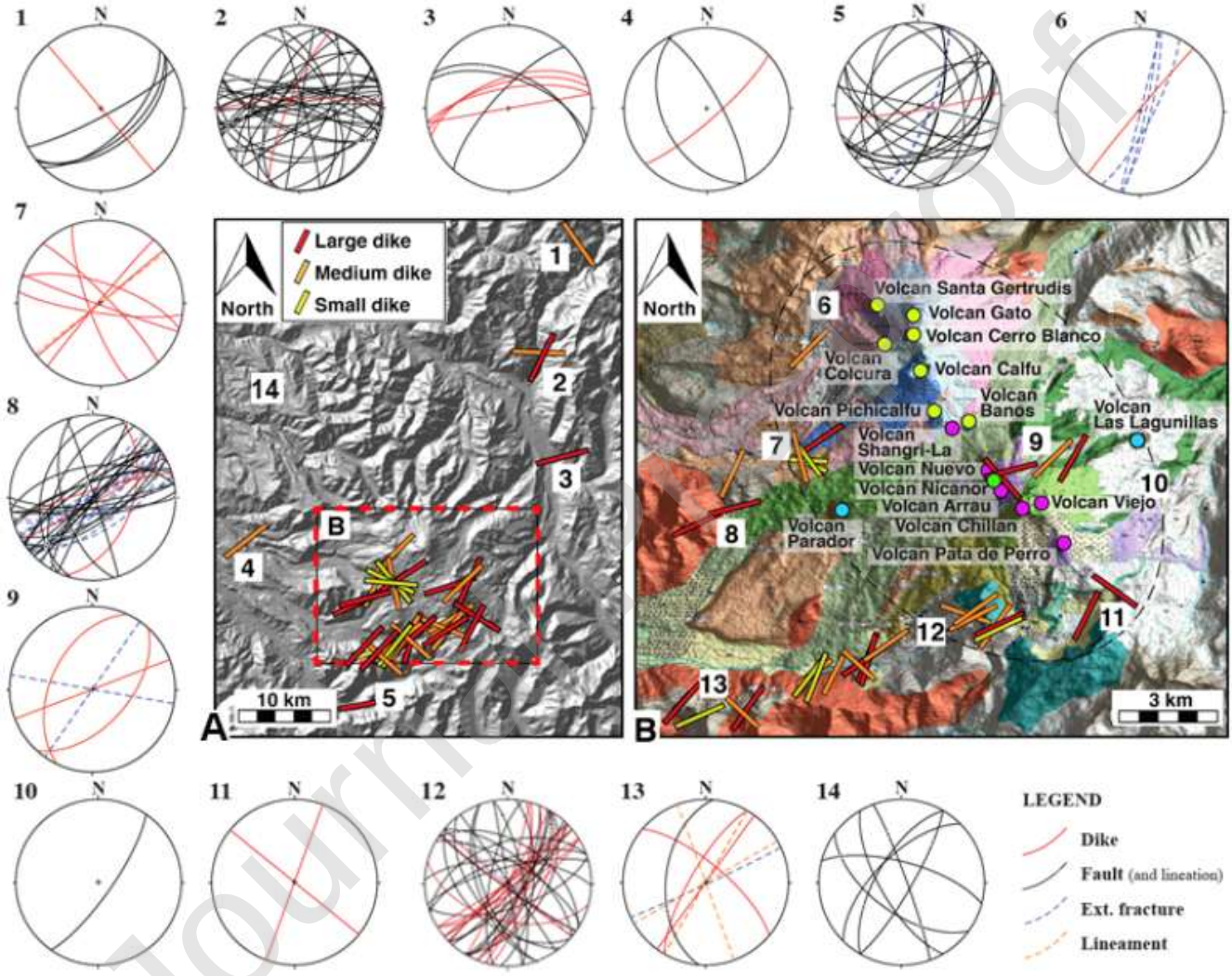

FIGURE 2

Structural sites of the area investigated during the field analysis. The orientation of the dikes shows a dominant NE-striking direction. The numbers refer to the stereoplots around the maps. Panel B shows the close up framed in panel A. The coloured map of panel B is modified from the geological map of the Nevados de Chillán (Naranjo, et al., (2008)). For the age of the geological units refer to Naranjo et al., (2008).

Journal Pre-proof

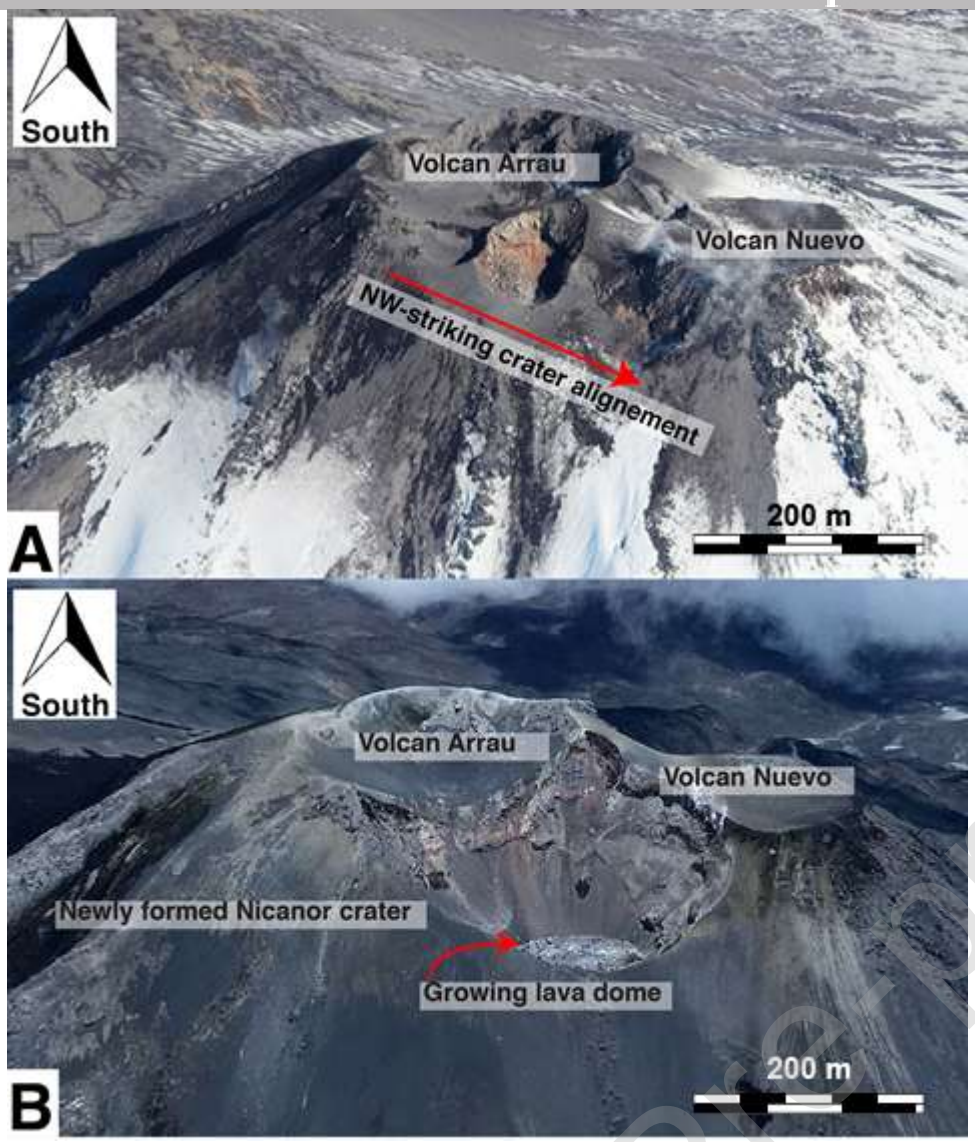

FIGURE 3

Evolution of the morphology of the summit of the Nevados de Chillián during the 2015-19 (ongoing) eruption. The three craters (panel A) initially aligned along a NW direction before merging into the newly formed Nicanor crater (panel B). The early phase of the eruption began by forming a NW oriented fissure-like row of craters. It should be noted that not every eruption of the Nevados de Chillián can and should be associated to a seismic event. For instance, the small NW oriented eruption occurred in 2003 between Volcan Nuevo and Arrau (Moussallam et al., 2018) cannot be associated to any major earthquake. Note that when considering fissure eruptions in the dataset we assume that the eruption was fed by dikes striking in the same direction of the mapped fissure.

Journal Pre-proof

Journal Pre-proof

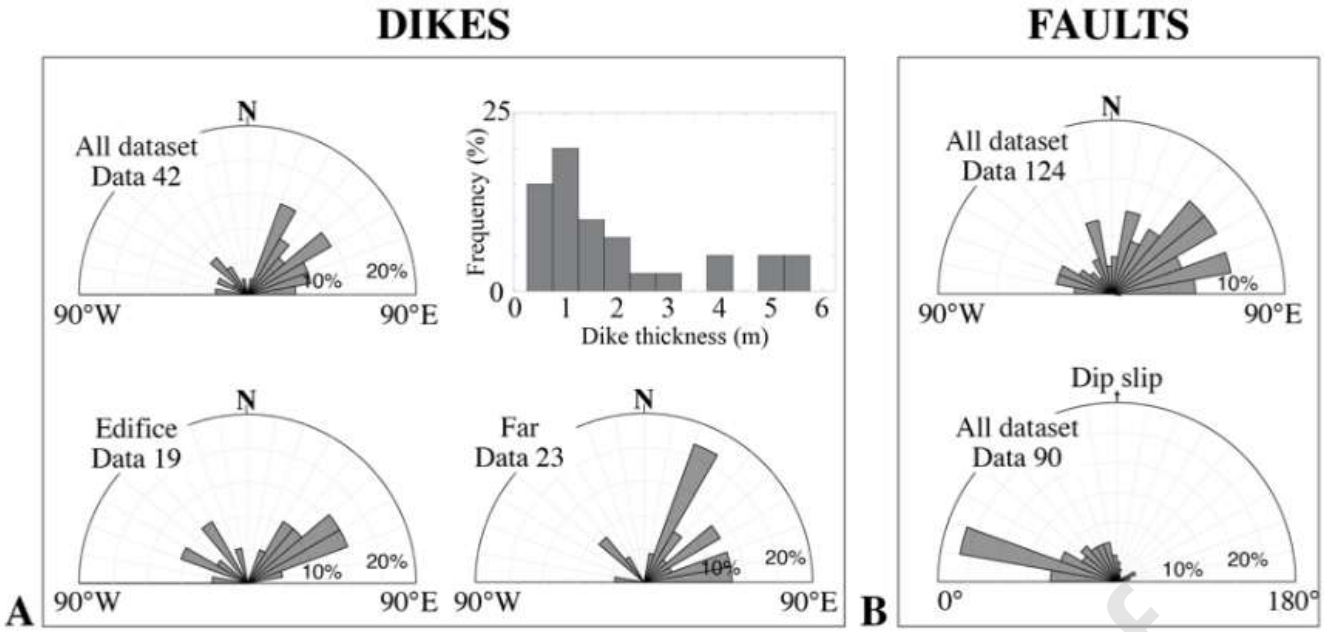

FIGURE 4

Rose diagrams of the mapped geological structures. Dikes and faults are shown in panel A) and B), respectively. The panels of B) show the frequency of fault strikes and direction of kinematic indicators (groves, slicke slides, etc.) on the fault plane (for 0° and 180° the fault is purely strike slip, for 90° is purely dip-slip). Note that we exclude that any of the fault measured was reactivated by the Maule earthquake, as there were no signs of rupture described in this region after this event. Additionally, the faults that we measured had large displacements (i.e. not possible to be accumulated in a short timespan) and none of the fault planes we examined was fresh.

Journal Pre-proof

Journal Pre-proof

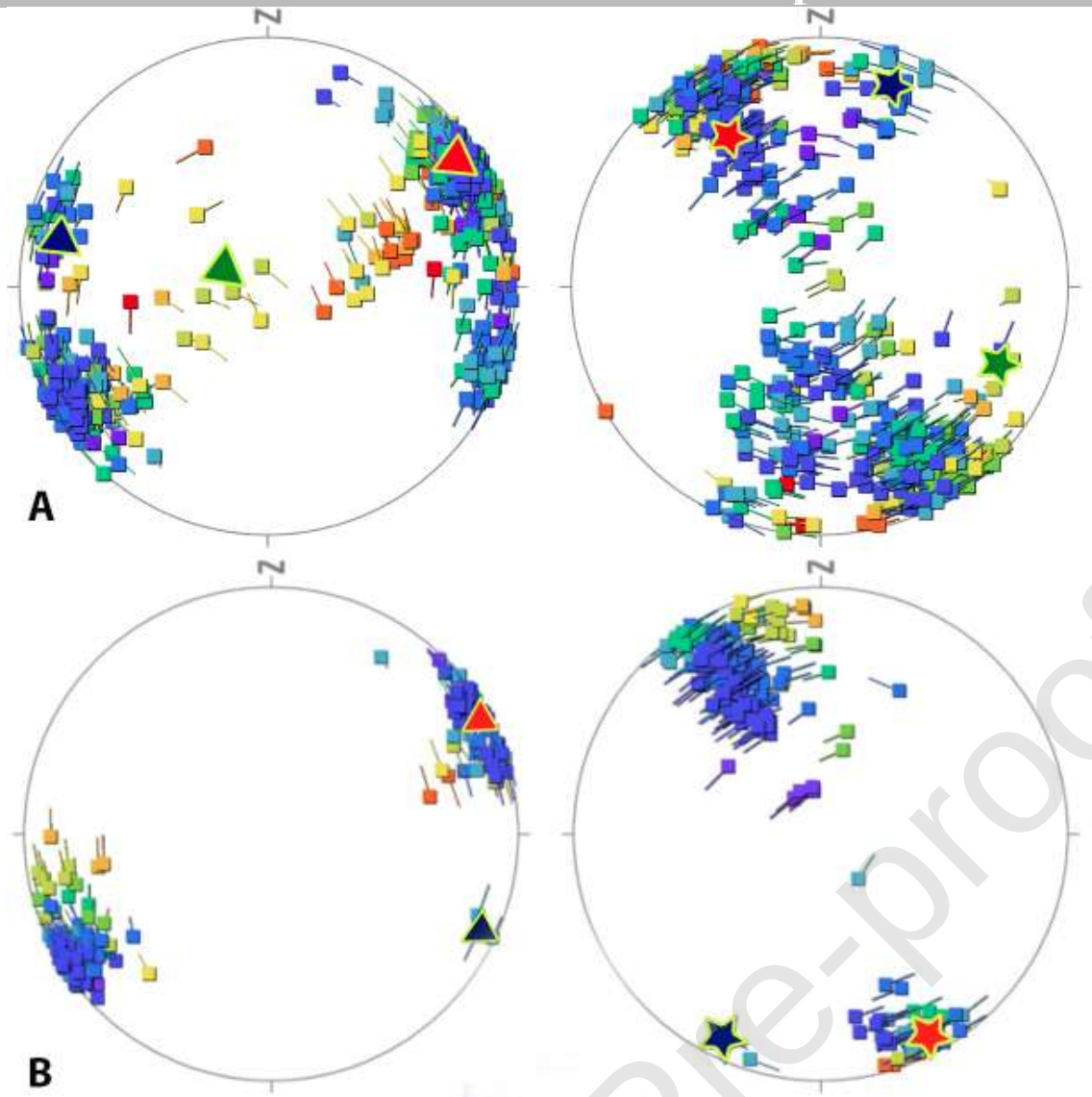

FIGURE 5 Orientation of the maximum and minimum stress tensors retrieved from fault data. Triangles indicate σ_1, stars σ_3. Red, blue and green indicate the three regimes described in the main text (i.e. NE-, NW- and E-W-oriented σ_1). Panel A) shows the entire fault dataset. The analysis of the kinematic data points out 3 possible clusters. The most abundant cluster (red) describes a transpressional regime (φ=0.1, σ_1 N57,9° dip 7,9° and σ_3 N323° dip 31.6°), the second cluster (blue) (φ =0.2, σ_1 N284.4° dip 18.3° and σ_3 N17.9° dip 10.6°) also indicates transpression. The third and least abundant cluster (green) shows extension (φ =0.6, σ_1 N287.6° dip 73.9° and σ_3 N109.7° dip 16.1°). Panel B) shows only data collected in the volcanic edifice. The data were inverted with Faultkin software from Yamaji (2000).

Journal Pre-proof

Journal Pre-proof

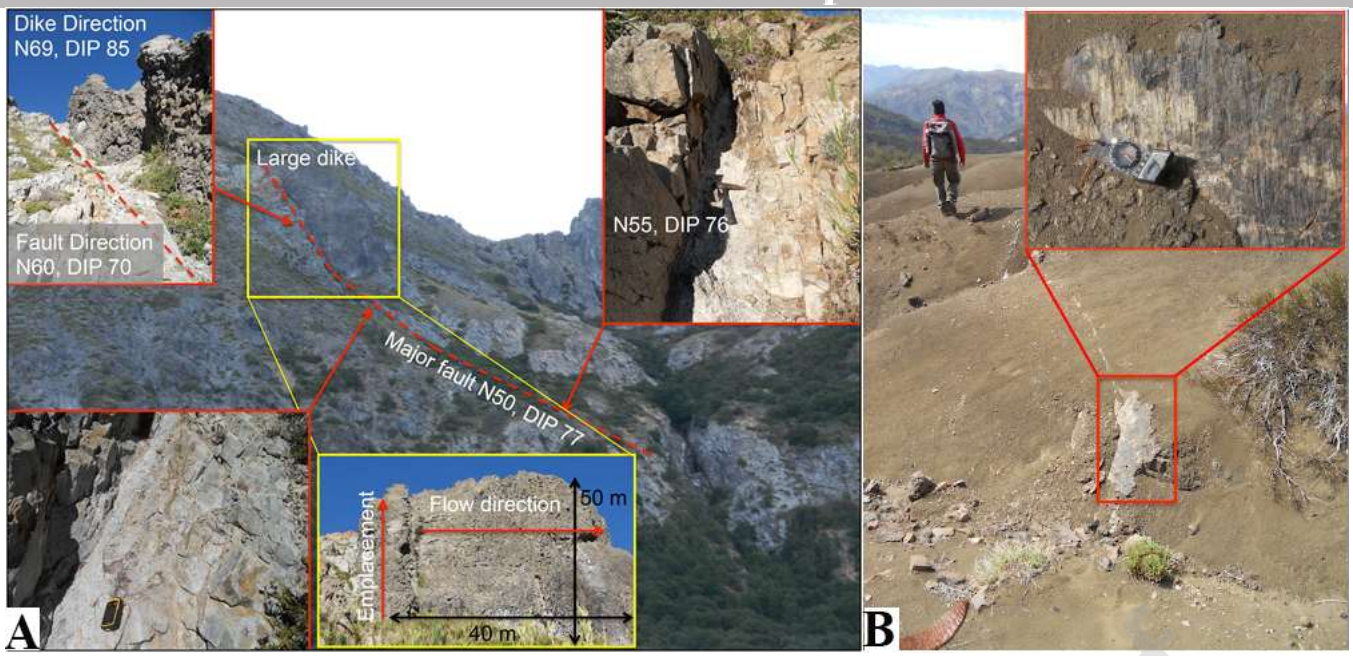

FIGURE 6

Faults recognised in the field. Panel A) shows the association between a fault and a dike observed in the field. Well-developed fault systems are often associated with the occurrence of a magmatic structure intruded along the fault plane. The damage zone of the fault can be followed for more than 200 m uphill. At the top of the hill a dike intruded in the damage zone fed an effusive eruption. Panel B) points out one of the normal faults mapped around the NdCVC. The lineations and the rugosity of the fault plane show a normal sense of shear.

Journal Pre-proof

Journal Pre-proof

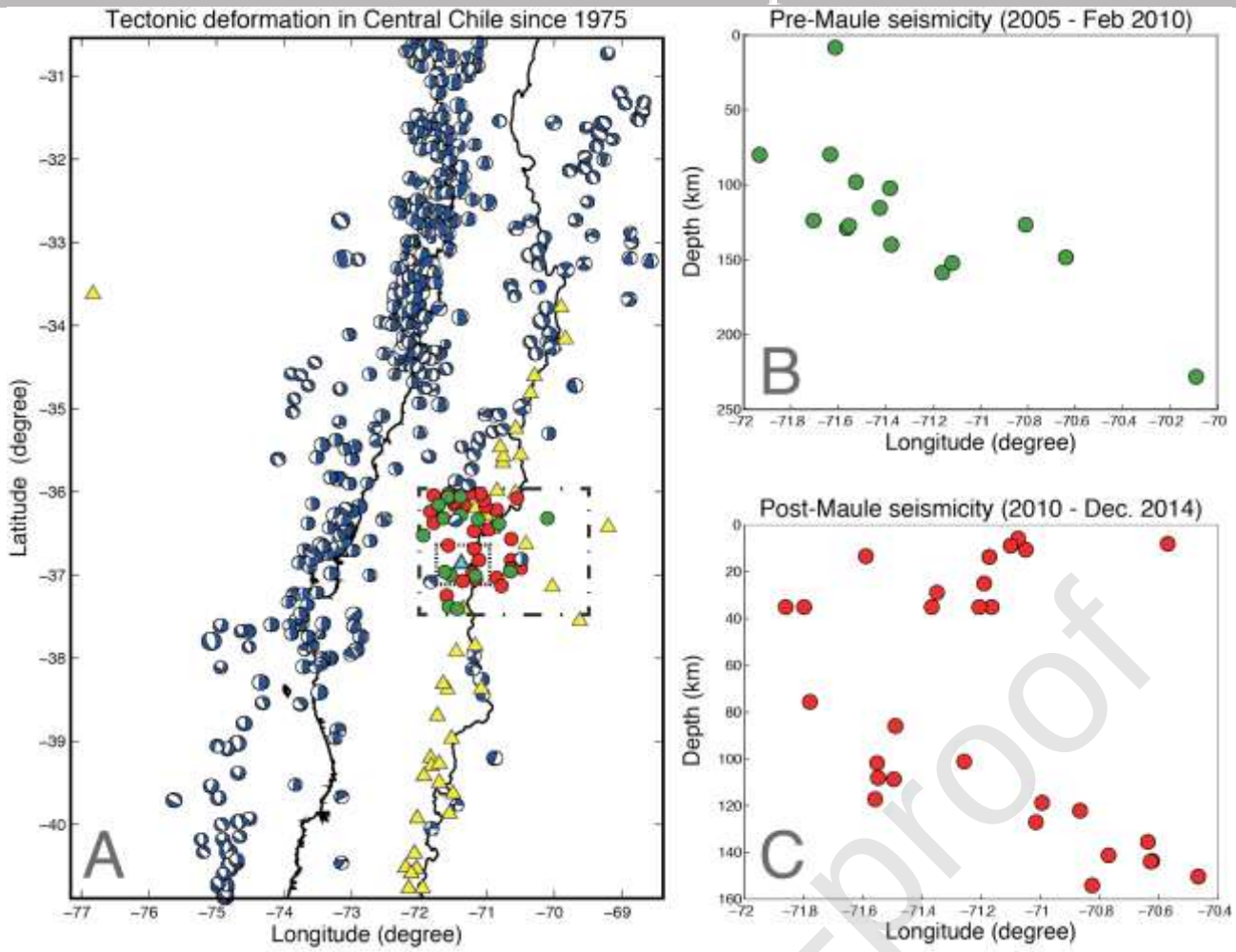

FIGURE 7

Seismic activity in Central Chile since 1975. A) The beach balls (retrieved from https://globalcmt.org) show the distribution of middle to large earthquakes highlighting an overall compressional regime, typical of convergent margins. B) Seismic activity beneath the volcanic arc (i.e. M≥4.0) before the Maule earthquake. Note that the seismicity is distributed almost only along the subduction interface. C) Post-Maule earthquake distribution (M≥4.0) below the volcanic arc in central Chile. Note the larger amount of shallow seismic events in the upper crust compared to panel B. The earthquakes were not re-localised and we rely on the locations of the CMT and USGS catalogues assuming that for a regional-scale study few kilometres errors are acceptable. The small and the large rectangles show the regions shown in Figures 2 and 8, respectively. The panels B) and C) show the projection of the earthquakes falling on the large rectangle of panel A) on a E-W-running cross-section.

Journal Pre-proof

Journal Pre-proof

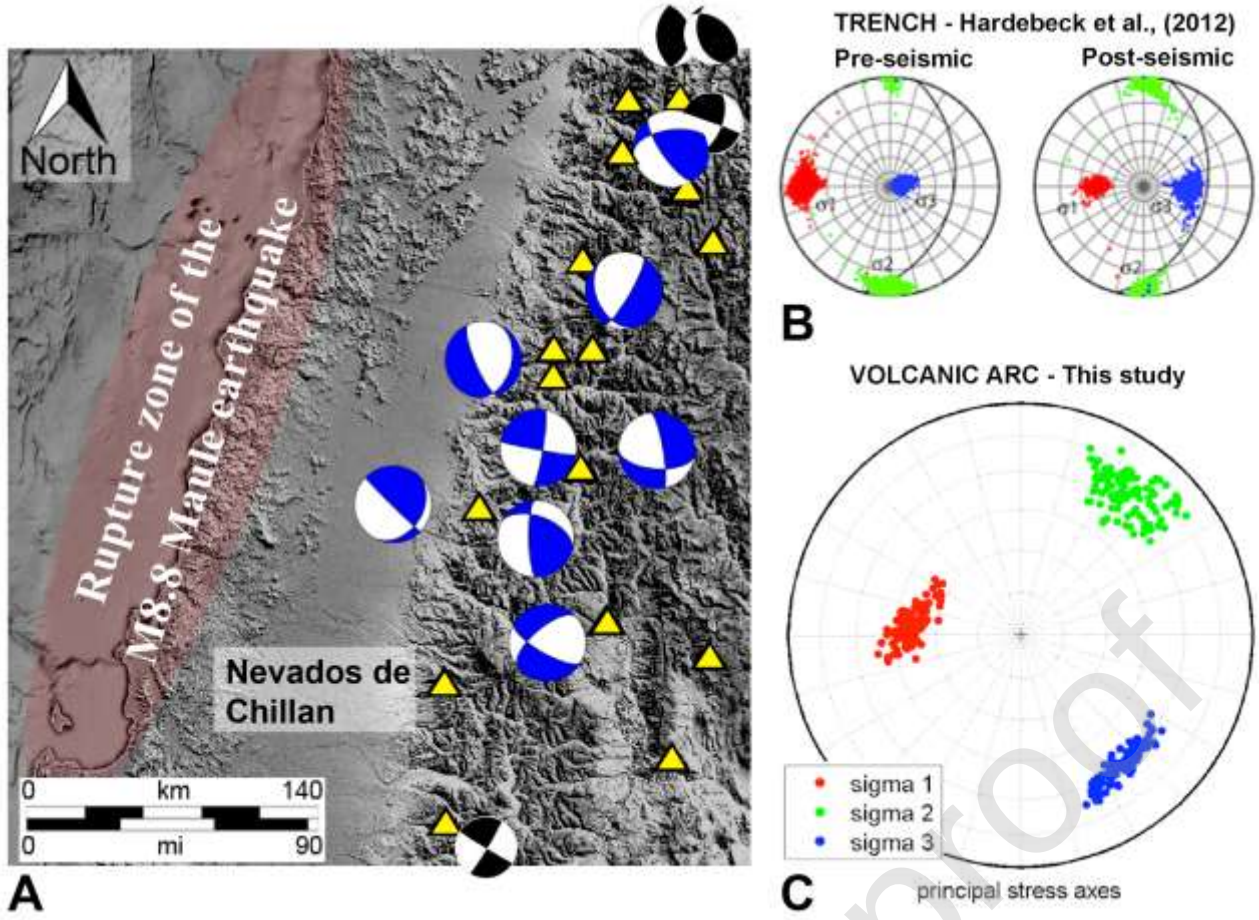

FIGURE 8

Focal mechanisms of seismic activity after the Maule earthquake and confidence limits of the principal stress tensors. We inverted the shallow (i.e. less than 35 km deep) middle- to large-magnitude earthquakes (i.e. M≥4.0) after the Maule earthquake recorded by the network of Gonzalez et al., (2018). Refer to Table 1 for more information about the seismic events. Panel A) shows the focal mechanisms of the earthquakes that we could invert (blue beach balls) compared to the focal mechanisms reported by Cembrano and Lara, (2009) and Sielfeld et al., (2019) (black beach balls). The network that was used to retrieve the waveforms is described by Gonzalez et al., (2018). Note that we present inversion only for the events that showed stable solutions. B) Confidence limits of the computed principal stresses for inter- and post-seismic periods shown by Hardebeck (2012) for the trench before and after the Maule earthquake. C) Confidence limits of the computed principal stress directions for the major seismic events during post-seismic periods below the volcanic arc (i.e. blue events of panel A). The confidence limits of the principal stress tensors were calculated using the software *stressinverse* (Vavryčuk, 2014). Following Vavrycuk (2014) the number of points in the sigma plot is large (i.e. larger than the number of inverted events) because, they result from repeating stress inversions. This is necessary considering the low amount of available focal mechanisms. The scatter of points gives an idea about the errors of the sigma directions. The true solution lies somewhere inside the cluster.

Journal Pre-proof

Journal Pre-proof

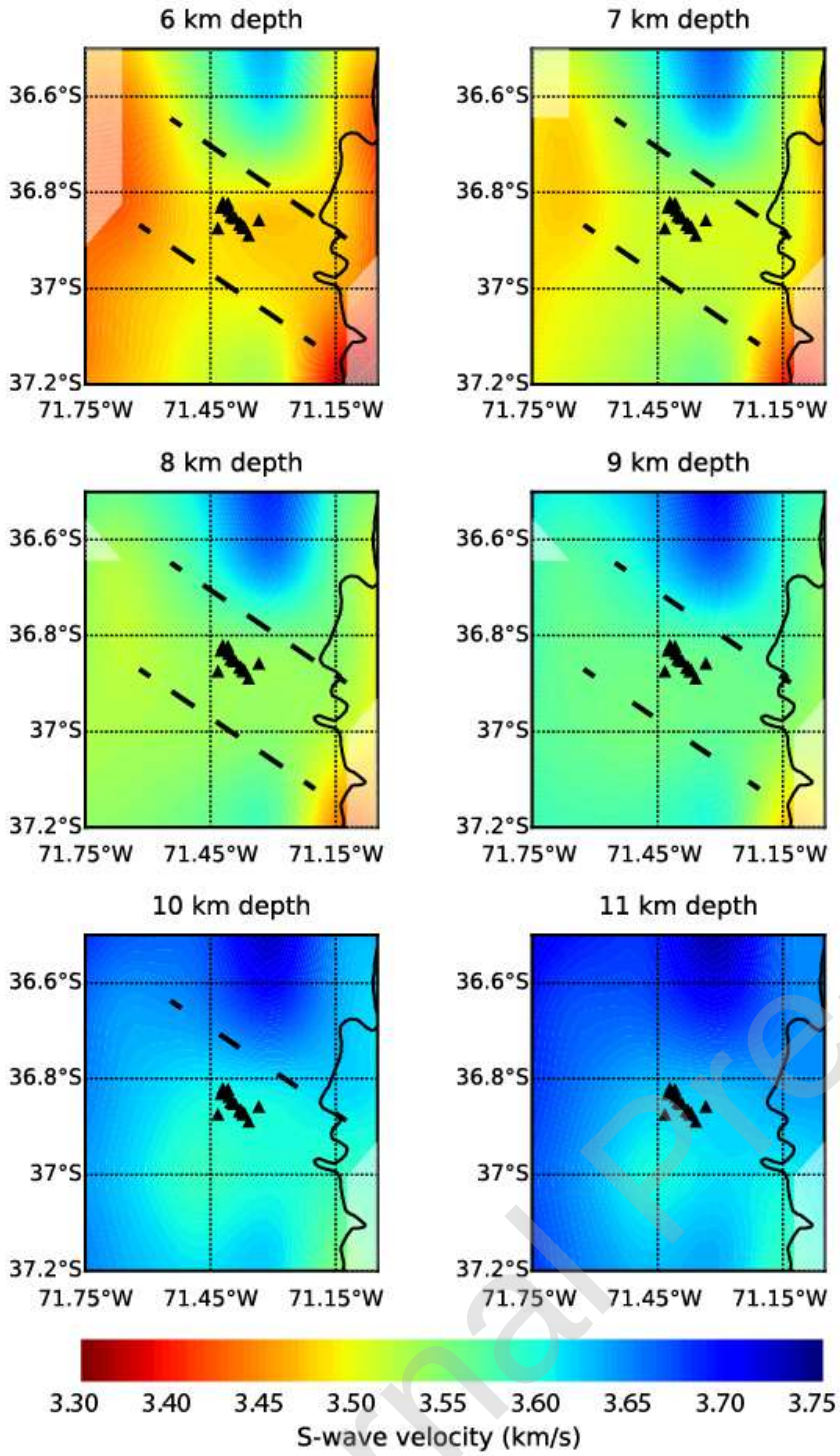

FIGURE 9

Distribution of shear wave velocities beneath the Nevados de Chillán volcanic complex. The black triangles point out the location of the cones shown in Figure 2. The inverted shear wave velocities seem to follow a NW-striking direction. This NW-trend is bounded by black dashed lines that become more and more spaced with increasing depth to indicate that the anomaly is progressively less visible. The shear wave velocities are provided by Gonzalez et al., (2018) who already discussed the methods to extract absolute shear wave anomalies from ambient noise. The reader is referred to Gonzalez et al., (2018) for further information about the ambient noise method used for this inversion.

Journal Pre-proof

Journal Pre-proof

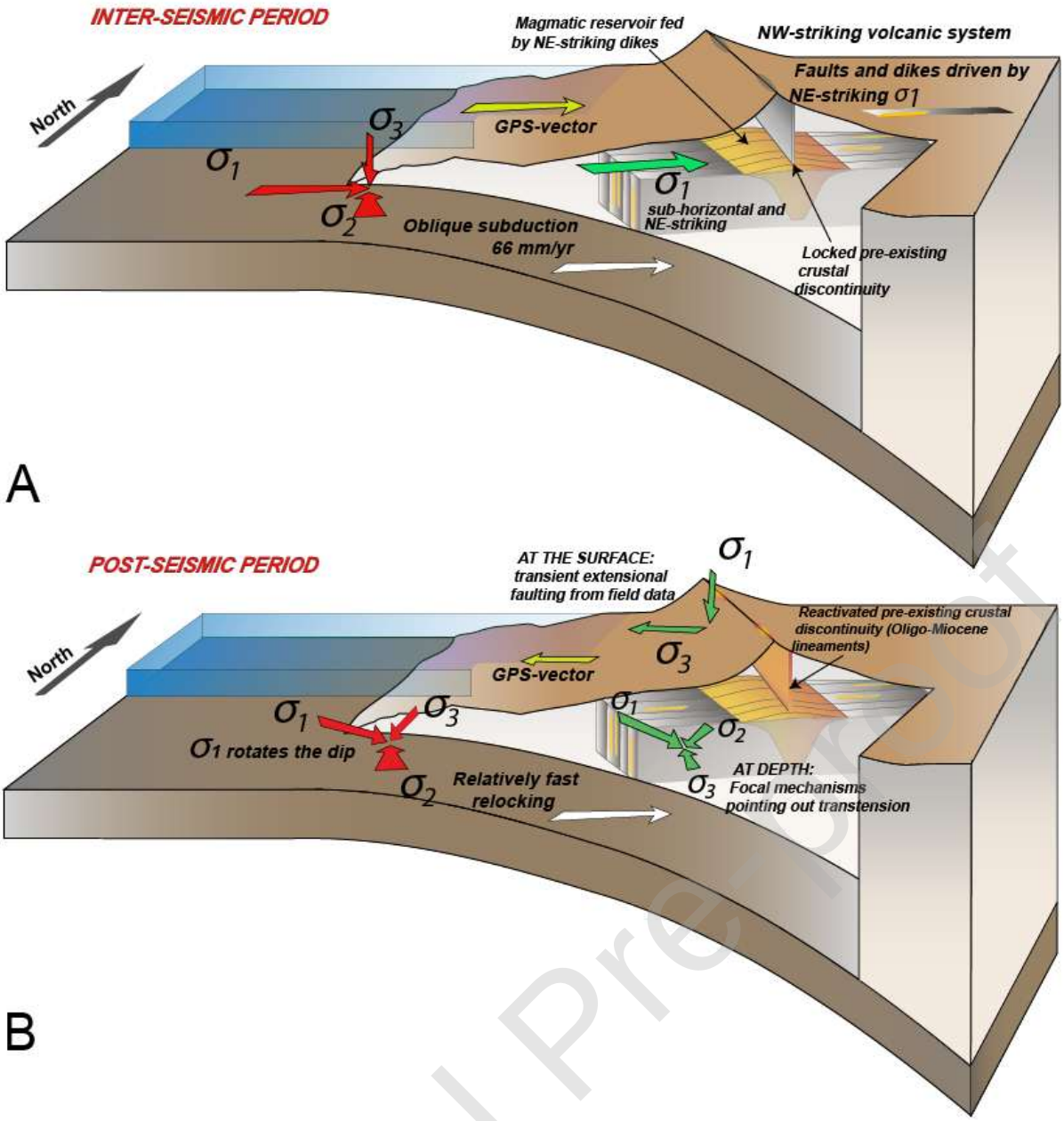

FIGURE 10

Conceptual model for the development of NW-striking volcanic systems in the Southern Central Andes. During inter-seismic periods (panel A) the principal stress tensors in the trench point out a compressional environment. In the arc the tectonic regime promotes the development of NE-striking structures that may feed the deep magmatic reservoir. The GPS vectors (yellow arrow) point out a landwards motion (e.g. Moreno et al., (2010)). After the megathrust earthquake (panel B) the direction and dip of the principal stress tensors σ_1 becomes inclined both in the trench (Hardebeck (2012) and in the volcanic arc (this study, Figure 8c). Field data indicate the occurrence of an extensional regime. The inversion of the focal mechanisms also indicates some extension (i.e. transtension). Note that the model is not to scale. Red and green arrows indicate the orientation of the stress tensors in the trench and below the volcanic arc, respectively.

Journal Pre-proof

Journal Pre-proof

TABLE 1. List of M>M4.0 earthquakes shallower than 35 km occurred in the volcanic arc after the M8.8 Maule earthquake. In grey the focal mechanisms of the events shown in Figure 8.

Date			Latitude	Longitude	Depth		M
2/27/2010	9:25:18	UTC	37.701 S	71.837 W	35	km	4.9
2/27/2010	9:34:53	UTC	35.714 S	71.105 W	35	km	4.3
2/27/2010	14:18:40	UTC	35.786 S	70.561 W	35	km	4
2/27/2010	23:46:09	UTC	35.467 S	70.285 W	35	km	4.5
2/28/2010	1:52:00	UTC	36.177 S	71.359 W	35	km	4.2
3/1/2010	10:17:25	UTC	37.071 S	71.367 W	35	km	4.8
3/5/2010	8:15:53	UTC	36.990 S	71.207 W	35	km	4.4
3/5/2010	8:21:26	UTC	37.067 S	71.165 W	35	km	4
3/20/2010	1:41:07	UTC	37.825 S	71.664 W	35	km	4.5
4/3/2010	3:38:19	UTC	35.324 S	70.339 W	6.3	km	4.4
5/29/2010	17:15:11	UTC	35.454 S	70.256 W	10	km	4.1
8/15/2010	7:50:36	UTC	36.814 S	71.101 W	8.9	km	5.2
8/15/2010	7:50:36	UTC	36.820 S	71.080 W	10	km	5.2
9/6/2010	10:47:45	UTC	35.322 S	70.491 W	13.4	km	4.5
1/21/2011	10:25:22	UTC	37.692 S	71.907 W	17.5	km	4.8
2/18/2011	23:54:03	UTC	34.910 S	70.390 W	17.7	km	4.8
6/7/2012	19:25:25	UTC	36.036 S	71.075 W	5.8	km	5
6/7/2012	4:05:04	UTC	36.074 S	70.570 W	8	km	6
7/14/2012	22:34:40	UTC	36.077 S	71.050 W	10.5	km	4.8
11/29/2012	20:40:59	UTC	36.426 S	71.082 W	3.3	km	4.2
11/14/2013	4:20:57	UTC	36.700 S	71.190 W	25	km	4

Journal Pre-proof